이학석사 학위논문

JAK-STAT signaling in breast cancer cell regulates paclitaxel sensitivity by tumor micro-environment interactions

유방암 세포에서 JAK-STAT signaling에 의한 종양 미세환경의 조절 및 paclitaxel의 감수성에 관한 연구

2020년 2월

서울대학교 대학원

협동과정 종양생물학 전공

한 종 민

JAK-STAT signaling in breast cancer cell regulates paclitaxel sensitivity by tumor micro-environment interactions

유방암 세포에서 JAK-STAT signaling에 의한 종양 미세환경의 조절 및 paclitaxel의 감수성에 관한 연구.

February 2020

Seoul National University

Cancer Biology

Jong-Min Han

Abstract

JAK-STAT signaling in breast cancer cell regulates paclitaxel sensitivity by tumor micro-environment interactions

Jong-Min Han

Cancer Biology

The Graduate School

Seoul National University

Breast cancer is consistently the cancer type that makes up the highest proportion of cancers in women worldwide. Triple negative breast cancer (TNBC) is the most malignant and difficult to treat. Although most hormone therapies target one of three receptors in other breast cancer subtypes, TNBC does not have any targeting molecule. Therefore, triple negative breast cancers (TNBCs) often require chemotherapy. Paclitaxel is a well-known chemotherapeutic agent for breast cancer, but patients often

acquire resistance to paclitaxel during chemotherapy. To understand the mechanism of paclitaxel resistance that occurs in TNBC tumors, response to paclitaxel experiment was performed using seven xenograft models derived from patients with TNBC *in-vivo* . For each TNBC PDX model, 10 mice were intraperitoneally injected with either PBS (Vehicle) or paclitaxel (15 mg/kg) for 4 weeks. Of the seven PDX models, the four that did not experience a reduction in tumor size by paclitaxel were designated as the paclitaxel-resistant group. The three PDX models whose tumor sizes were significantly reduced by paclitaxel were designated as the paclitaxel-sensitive group. Then, transcriptome sequencing data from both groups were analyzed. JAK-STAT pathway-related genes were identified among the many genes with increased expression levels in the paclitaxel-resistant group compared to the paclitaxel-sensitive group. Therefore, the correlation between the upregulation of the JAK-STAT pathway and paclitaxel resistance was the focus of this study. It was further observed that paclitaxel and ruxolitinib (JAK1/JAK2 inhibitor) combination treatment in five TNBC cell lines has a synergistic effect on anti-cancer activity. When JAK2 gene knockdown by JAK2 siRNA occurred in four TNBC cell lines *in*

vitro, JAK2 inhibition TNBC cell lines were found to be more sensitive to paclitaxel. Additionally, the paclitaxel-resistant tumors upregulated the cell cycle-related genes in the tumor microenvironments. Therefore, tumor microenvironments, such as fibroblasts and endothelial cells, were found to have upregulated proliferation in the tumors of mice in the paclitaxel-resistant group. And it was confirmed that proliferation decreased in fibroblasts incubated in CM extracted from JAK2-inhibited TNBC cell lines. The results of this study demonstrate that paclitaxel resistance in TNBC is correlated with various genomic changes and the upregulation of the JAK-STAT pathway. Further studies are essential to clarify the mechanistic pathways of the JAK-STAT pathway correlated with paclitaxel resistance.

Key words: Paclitaxel, ruxolitinib, resistance, JAK-STAT pathway, TNBC.

Student Number: 2018 - 27894

Contents

List of Tables

List of Figures

Introduction

Breast cancer is the most common cancer among the woman, and the incidence of breast cancer is steadily rising in Korea. [1] Breast cancer is commonly divided into four subtypes; luminal A, luminal B, HER2 positive, and TNBC. Unlike other subtypes of breast cancer, TNBC is characterized by the absence of ER, PR and HER2.[2] TNBC is the most malignant and difficult to treat breast cancer subtype as most hormone therapies target one of the three receptors, while TNBC does not have a target molecule for treatment. Therefore, TNBCs often require chemotherapy. [3] Although TNBCs account for approximately 15-20% of breast cancers, the recurrence and fatality rates of this subtype are significantly worse than those of others.[4]

Paclitaxel is used to treat various types of solid tumors, including ovarian, breast, lung, and prostate cancers.[5] The best known anti-cancer mechanism of paclitaxel is by targeting of the microtubule.[6] In addition, stabilization of the microtubules and consequently, cell cycle arrest occur in G2-M phase. Paclitaxel also induces multi-polar spindle in cancer cells that

are associated with apoptotic effect. [5, 7, 8] Although, paclitaxel has been shown to be successful in preclinical and clinical studies, the intrinsic or acquired paclitaxel resistance remains a challenge in cancer treatment. [9–12]

The JAK /STAT signaling pathway is activated by various cytokines, interferons, growth factors and regulates many genes involved in cell proliferation, survival, differentiation. [13–15] The JAK/STAT signaling pathway is upregulated in many cancers to promote tumor growth and progression. In particular, both STAT3 and STAT5 promote breast cancer growth and progression. Therefore, the JAK/STAT pathway is currently being considered a potential therapeutic target for breast cancer. [16–23]

Ruxolitinib (Jakavi) is selective JAK1 and JAK2 inhibitor that was FDA–approved in November 2011 for the treatment of myelofibrosis, a type of myeloproliferative disorder that occurs in bone marrow. [24–27] The therapeutic effect of ruxolitinib has recently been evaluated clinically in ovarian, metastatic breast, and pancreatic cancers. [27–29]

In this study, four TNBC PDX models were identified that are relatively paclitaxel–resistant, and three that are paclitaxel–sensitive.

Therefore, TNBC PDX models that showed paclitaxel resistance or sensitivity were analyzed via RNA sequencing. The mRNA expressions of these samples upregulated the mRNA expression of the JAK-STAT pathway-related genes in tumors showing paclitaxel resistance. Therefore, it was assumed that the paclitaxel resistance was related to upregulation of the JAK-STAT pathway activity. *In-vitro* and *in-vivo* studies were performed to investigate the relationship between paclitaxel resistance and the JAK-STAT signaling pathway in TNBC.

Materials and methods

1. cDNA synthesis and qPCR

RNA was extracted from cells, that were then washed once with 1x PBS and prolonged by TRIzol (Favorgen, Taiwan). Prime Script 1st strand cDNA Synthesis Kit (Takara, Japan) was used for reverse transcription of RNA, and qPCR was carried out using Power SYBR Green PCR Master mix (Applied Biosystems). Reactions were performed using a real-time PCR System (ABI7500) and the results were analyzed with the comparative Ct to establish the relative expression curves. The sequence of the primer used for JAK2 was forward 5'-TCACCAACATTACAGAGGCCTACTC-3' and reverse 5'-GCCAAGGCTTTCATTAAATATCAAA-3'. The sequence of the primer used for STAT3 was forward 5'-GGCCCCTCGTCATCAAGA-3' and reverse 5'-TTTGACCAGCAACCTGACTTTAGT-3'. The sequence of the primer used for STAT5 was forward 5'-GTCACGCAGGACACAGAGAA-3' and reverse 5'-CCTCCAGAGACACCTGCTTC-3'.

2. Western blotting

Proteins were harvested with RIPA buffer (Thermo scientific, Palm Springs, CA, USA), protease and phosphatase inhibitor, and 0.5M EDTA solution. Protein concentrations were measured using BCA assay kit (Thermo scientific, Palm Springs, CA, USA). Cell lysates containing 20ug of protein were loaded onto 10% gels and transferred to a PVDF membrane. The membrane was blocked with 5% BSA solution and incubated with primary antibody overnight at 4'C. The second antibody was diluted 1:5000 in 5% skim milk. Bands were detected by LAS.

3. MTT cell viability assay

BT20, HCC38, HCC70, MDA-MB231, and MDA-MB468 cells were seeded into 96-well plates at a density of 3,000 cells per well. After overnight incubation, the attached cells were treated with various concentrations of paclitaxel, ruxolitinib, or a mixture of the two for 72h. The cells were incubated with MTT solution (5 mg/ml, 20μl/well) for 3h at 37℃. The medium was removed and 200μl DMSO was added to each well to

dissolve the formazan crystals in the viable cells. The optical density was determined at a wavelength of 570 nm using a spectaMAX190.

4. Immunohistochemistry (IHC)

IHC was performed with an IHC staining kit (Dako, CA, USA). Tissue sections were deparaffinized in xylene substrate, hydrated in phosphate buffered saline (PBS), and blocked with normal goat serum (AAR-6591-02, Immuno bioscience). Slides were incubated with primary antibody (1:1000 or 1:2000) at 4℃ overnight. The next day, the tissue sections were incubated with biotinylated anti-rabbit/mouse antibody, followed by exposure to preformed avidin/biotinylated peroxidase solution. Sections were then developed with diaminobenzidine and hydrogen peroxide, which produces a brown precipitate. Sections were counterstained with hematoxylin, dehydrated, and mounted.

5. Cell culture

In this study, 11 breast cancer cell lines were used. The MCF-7, MDA-MB231, MDA-MB468, and HS578T cell lines were cultured in Dulbecco's modified Eagle's (DMEM) medium supplemented with 10% FBS and 1% penicillin/streptomycin at 37℃ under a humidified atmosphere of 5% CO2. The ZR-75-1, SKBR3, BT474, MDA-MB453, BT20, HCC38, and HCC70 cell lines were cultured in RPMI 1640 with 10% FBS and 1% penicillin/streptomycin at 37℃ under a humidified atmosphere of 5% CO2. All cell lines were sub-cultured every three to four days.

6. Transient transfection of JAK2 siRNA

Four human breast cancer cell lines (BT20, HCC38, MDAMB231, and MDA-MB468) were used in this study. Commercial JAK2 siRNA was obtained from Dharmacon Inc. and used to target human JAK2 (Gene ID:3717). Cells were transfected with siRNA (10nM) using the ON-TARGETplus Human JAK2 siRNA-SMARTpool siRNA transfection reagent, according to the manufacturer's instructions. Nonspecific siRNA

(Dharmacon Inc.) was used as a negative control, and the selective silencing of JAK2 was confirmed by western blot analysis.

7. Antibodies

The following antibodies were used: β-actin (sc-47778) from Santa Cruz; JAK2 (3230s), STAT3 (4904s), and STAT5 (9363s) from Cell Signaling; pJAK2 (ab219728), pSTAT3 (ab76315), pSTAT5 (ab32364), and KI-67 (ab15580) from Abcam.

8. In-vivo TNBC patients derived xenograft experiments

In-vivo, a paclitaxel response test was performed on a patient-derived xenograft model. Seven TNBC PDX models were established separately. For each model, vehicle (n = 5) and paclitaxel (n = 5) mice were intraperitoneally (IP) injected with either PBS or paclitaxel (15 mg/kg) for 4 weeks. After the experiment, four of the PDX models were found to have less response to paclitaxel compared to the other three models, and were designated as the paclitaxel non-responding group. Meanwhile, the three models that were more sensitive to paclitaxel were designated as the

paclitaxel responsive group. Transcriptome and exosome sequencing data were analyzed from the remaining TNBC PDX tumors.

9. Whole transcriptome sequencing and expression analysis

RNA sequencing libraries were prepared using a Truseq RNA kit, and sequenced on an Illumina HiSeq platform. STAR aligner [30] was used to align the sequence reads to the combined genome of the GRCh37/b37 human reference genome and mm10 mouse reference genome. We used htseq-count in the HTseq [31] package to obtain the number of reads for each gene. The read counts of the genes were converted to FPKM (Fragments Per Kilobase of transcript per Million read mapped) using the rpkm function from edgeR. [32]

A differential gene expression analysis was performed with DESeq2. [33] Genes with low read counts across all samples were excluded. Among the differentially expressed genes (DEGs) from the differential gene expression analysis, only genes with mean FPKM ≥ 1, adjusted P value < 0.05, and log2 FC(fold-change) ≥ 1 were retained. The DAVID (Database

for Annotation, Visualization, and Integrated Discovery) [34] functional annotation tool was used to identify significantly enriched pathways in the list of filtered DEGs. Hierarchical clustering was performed using cluster 3.0 [35] (log transformed FPKM, mean-centered, uncentered correlation, average linkage) and visualized using JAVA TreeView . [36]

10. Statistics

GraphPad prism 8 software (GraphPad Prism, USA) was used to carry out statistical analyses. For comparing means between two groups, a two-tailed Mann-Whitney t-test and multiple t-test were used (*: $p < 0.05$, **: $p < 0.01$, ***: $p < 0.005$,) (GraphPad Prism v. 8.02 software for Windows).

Results

Establishment of TNBC PDX models with paclitaxel resistance.

To understand what molecules affect cancer cells when paclitaxel resistance develops in triple negative cancer, *in-vivo* paclitaxel experiments were performed utilizing seven PDX models. Paclitaxel was administered for 4 weeks to seven PDX models of TNBC-derived tissues from passages 0 to 2. Then, the response to paclitaxel was confirmed in seven TNBC PDX tumors. In the four TNBC PDX models, X12, X61, X110, and MX158, there were no differences in tumor size reduction of the paclitaxel-treated tumors compared to the vehicle-treated tumors. However, the three TNBC PDX models of X125, X196, and X193 showed significant decreases in tumor size in paclitaxel-treated tumors compared to vehicle-treated tumors (Figure 1). Therefore, the four TNBC PDX models that did not experience a reduced tumor size because of paclitaxel were designated as the paclitaxel-resistant group, and the three PDX models whose tumor sizes were significantly reduced by paclitaxel were called the paclitaxel-sensitive group.

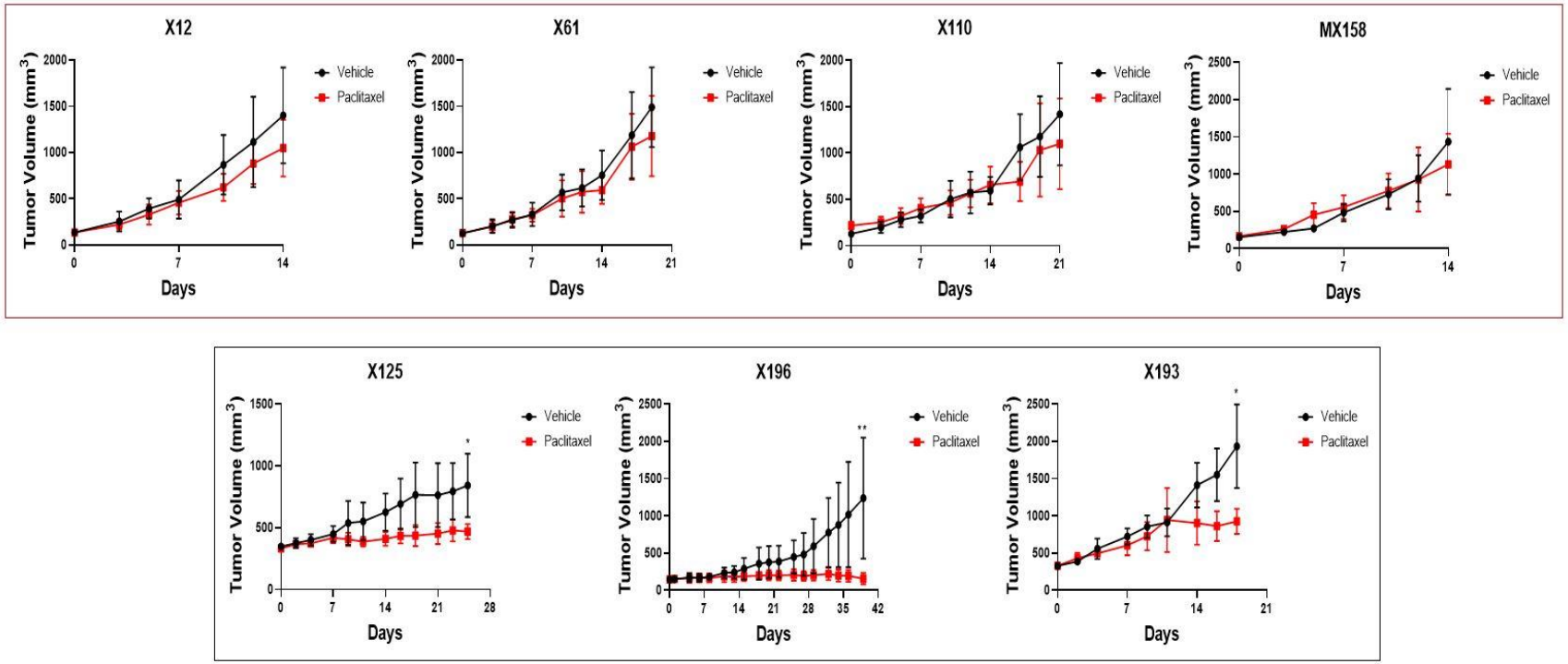

Figure 1. Response to paclitaxel in seven TNBC PDX models *in-vivo*. Seven PDX models were established from a single patient's primary or recurrent tumor. X110 is a recurred case of X61. The four TNBC PDX models (red boxed) that did not experience a

reduction in tumor size due to paclitaxel were designated as the paclitaxel-resistant group, and the three PDX models (black boxed) whose tumor sizes were significantly reduced by paclitaxel were called the paclitaxel-sensitive group. Data were expressed as mean ± standard deviation (SD). * $p \leq 0.05$; ** $p \leq 0.01$ (Mann-Whitney t-tes

The expression of JAK-STAT related genes is upregulated in paclitaxel resistance group.

Three out of five tumors were selected for each control and the paclitaxel group, and the transcriptome data were then obtained. Then, various genes showing differences in gene expression between the paclitaxel-resistant and -sensitive groups were analyzed. Transcriptome data showed differentially expressed genes (DEGs) between the paclitaxel-sensitive and resistant groups (Figure 2A). JAK-STAT pathway-related genes were upregulated in the paclitaxel-resistant group, but downregulated in the paclitaxel-sensitive group among the various genes showing differences in gene expression (genes with mean FPKM $\geq$ 1, adjusted P value $<$ 0.05, and log2 FC (foldchange) $\geq$ 0.8) between the paclitaxel-resistant and -sensitive groups (Figure 2B and Table 1). Surprisingly, the JAK-STAT pathway ranked fifth, following the pathways for NF-kappa B, TNF, cancer, and osteoclast differentiation in the paclitaxel-resistant compared to the -sensitive group. In particular, when five representative genes in the JAK-STAT pathway-related genes were analyzed between the paclitaxel-sensitive and -resistant groups using

FPKM values, the expression levels of JAK1, JAK2, and STAT5A were found to be significantly increased in the paclitaxel resistant group. However, STAT3 and STAT5b showed no difference between the paclitaxel-sensitive and -resistant groups (Figure 2C). Therefore, we hypothesized that resistance to paclitaxel may be associated with an upregulation of the JAK-STAT signaling pathway.

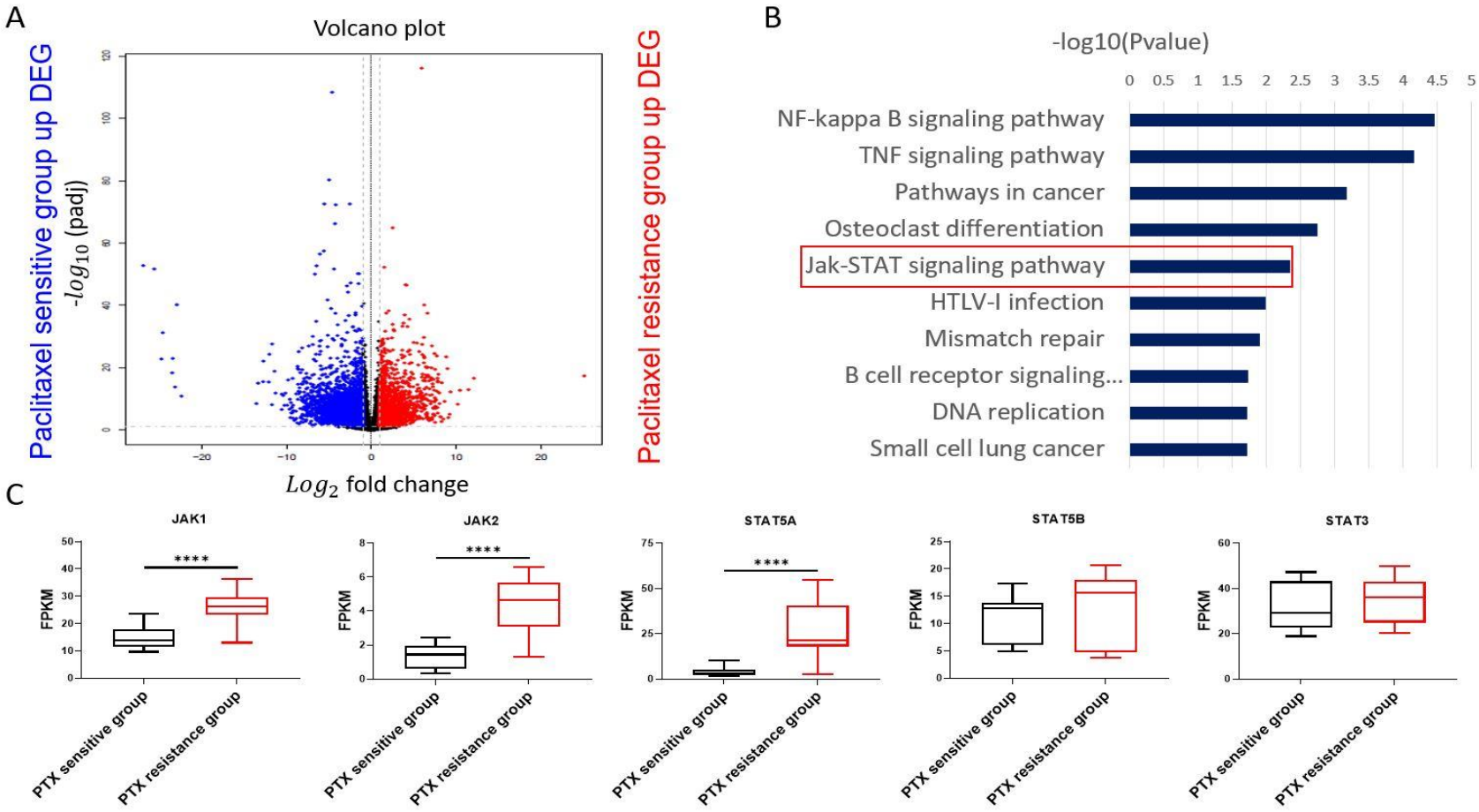
A
Volcano plot
Paclitaxel sensitive group up DEG
Paclitaxel resistance group up DEG
$-log_{10}$ (padj)
Log_2 fold change
B
-log10(Pvalue)
0 0.5 1 1.5 2 2.5 3 3.5 4 4.5 5
NF-kappa B signaling pathway
TNF signaling pathway
Pathways in cancer
Osteoclast differentiation
Jak-STAT signaling pathway
HTLV-I infection
Mismatch repair
B cell receptor signaling...
DNA replication
Small cell lung cancer
C
JAK1
JAK2
STAT5A
STAT5B
STAT3
FPKM
****
PTX sensitive group
PTX resistance group

Figure 2. Changes in JAK-STAT signaling pathway-related gene expression in paclitaxel-resistant groups in transcriptome analysis. (A) Volcano plot showing DEGs between the paclitaxel-sensitive and -resistant groups. The standard is a log2FC (fold-change) value of 1.0. Red points indicate genes upregulated in the paclitaxel-resistant group. Blue points represent genes upregulated in the paclitaxel-sensitive group. (B) The top ten pathways significantly enriched in the paclitaxel-resistant group using the list of filtered DEGs. (C) Differences in the expression of representative genes among the JAK-STAT pathway-related genes between the paclitaxel-sensitive and -resistant groups. JAK1, JAK2, and STAT5A, but not STAT5b or STAT3, were significantly upregulated in the paclitaxel-resistant group. **** $p \leq 0.0001$ (Mann-Whitney t-test).

Table 1. Upregulation of the pathways in paclitaxel-resistant tumors in comparison with those in paclitaxel-sensitive tumors based on DEG data.

Pathway	P-Value	Genes
NF-kappa B signaling pathway	3.44E-05	TRAF1, PTGS2, RELB, BCL2A1, TNFRSF13C, CD40, NFKB2, BIRC3, VCAM1, TNFRSF11A, TNFSF13B, PLCG2, TNFAIP3, BLNK
TNF signaling pathway	7.05E-05	TRAF1, PTGS2, CSF1, CXCL2, PIK3CD, IL15, BIRC3, JUNB, VCAM1, RPS6KA5, TNFRSF1B, BCL3, CREB3L1, FAS, TNFAIP3
Osteoclast differentiation	6.69E-04	CSF1, NCF4, PPARG, RELB, PIK3CD, MITF, SOCS1, NFKB2, JUNB, TYK2, CYBA, TNFRSF11A, PLCG2, NFATC1, BLNK
Pathways in cancer	0.001803749	WNT5A, TRAF1, PTGS2, STAT5A, MITF, PPARG, LPAR1, NFKB2, CCNE1, CXCR4, RASGRP1, TGFA, RARB, FAS, LAMB1, FGF3, CSF2RA, BMP4, TCF7, PIK3CD, BIRC3, DAPK2, NRAS, LAMA1, FZD10, LAMA4, GNAQ, PLCG2, VEGFA
Cytokine-cytokine receptor interaction	0.004546104	CSF1, CCR1, TNFRSF13C, LIFR, IL6R, CD40, IL15, KDR, TNFRSF1B, TNFRSF11A,, TNFSF13B, CXCR4, VEGFA, CSF2RB, IL2RG, FAS, BMP7, CSF2RA, BMPR1A
VEGF signaling pathway	0.010163248	NRAS, PLA2G4A, PTGS2, PIK3CD, PLCG2, VEGFA, SPHK1, KDR
Jak-STAT signaling pathway	0.012587523	PTPN6, STAT5A, PIK3CD, SOCS1, LIFR, IL6R, IL15, TYK2, STAT4, CSF2RB, IL2RG, CSF2RA, IL13RA2
Leukocyte transendothelial migration	0.018760643	VCAM1, CYBA, CXCR4, CLDN6, NCF4, BCAR1, PIK3CD, PLCG2, CLDN10, ITGB2, CLDN23
B cell receptor signaling pathway	0.019232406	NRAS, PTPN6, NFKBIE, PIK3CD, PLCG2, PIK3AP1, BLNK, NFATC1
Small cell lung cancer	0.019322564	TRAF1, CCNE1, LAMA1, LAMA4, PTGS2, PIK3CD, RARB, BIRC3, LAMB1
Protein digestion and absorption	0.023322131	KCNN4, ATP1B1, COL9A2, COL14A1, COL27A1, ACE2, PRSS1, COL11A1, SLC1A1
Amoebiasis	0.024844106	SERPINB9, LAMA1, LAMA4, SERPINB6, GNAQ, COL27A1, PIK3CD, ITGB2, LAMB1, COL11A1

Hepatitis B	0.029399943	CCNE1, NRAS, IKBKE, EGR3, STAT4, IFIH1, STAT5A, PIK3CD, CREB3L1, FAS, CCNA1, NFATC1
Other types of O−glycan biosynthesis	0.033158656	ST6GAL2, FUT7, GXYLT2, FUT4, GXYLT1

Protein expression levels associated with the JAK-STAT pathway are upregulated in tumors of the paclitaxel-resistant group.

The transcriptome investigations confirmed whether the increase of JAK-STAT pathway-related genes was upregulated by the protein expression levels. Therefore, the JAK-STAT pathway-related protein expression levels were analyzed by western blotting between paclitaxel-resistant and -sensitive TNBC PDX tumors (Figure 3A). One vehicle- or paclitaxel-treated individual was selected from each of the seven TNBC PDX models, and the proteins were extracted from the tumor to compare JAK2, STAT3, and STAT5 protein expression levels. Consequently, the protein expression levels of total JAK2, STAT3, and STAT5 were increased in the paclitaxel-resistant group compared to the paclitaxel-sensitive group. Differences in the protein expression levels of total STAT3 and STAT5 were statistically significant (Figure 3B).

In addition, there was no difference in the protein expression levels of JAK2, STAT3, and STAT5 between the paclitaxel-sensitive and -resistance tumors when treated with vehicle (Figure 3C). However, the

protein expression levels of JAK2, STAT3, and STAT5 were upregulated in the paclitaxel-resistant compared to the paclitaxel-sensitive tumors when treated with paclitaxel (Figure 3D). These results suggest that paclitaxel increased the expression levels of proteins related to the JAK-STAT pathway in the paclitaxel-resistant group and, therefore, the JAK-STAT pathway is found to be related to paclitaxel resistance in TNBC.

In addition, to determine whether the JAK-STAT pathway was activated, the protein expression levels of pJAK2 were analyzed through IHC staining (Figure 4). when IHC was conducted, the protein expression levels of pJAK2 declined in paclitaxel-sensitive TNBC tumors, but was upregulated in paclitaxel-resistant TNBC tumors. Consequently, it was confirmed that paclitaxel resistance is related to the activation of the JAK-STAT signaling pathway in TNBC.

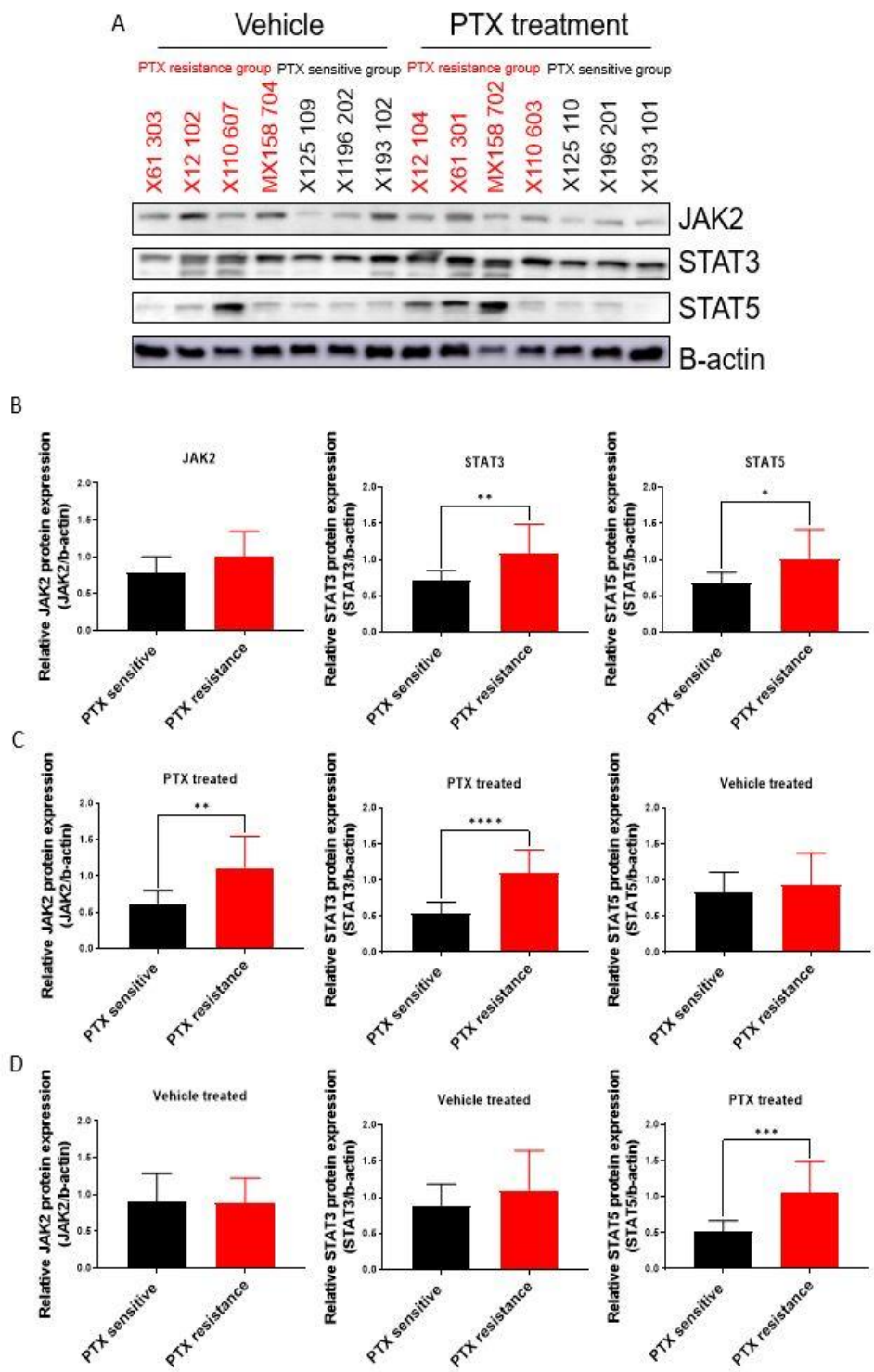
A
Vehicle
PTX treatment
PTX resistance group
PTX sensitive group
PTX resistance group
PTX sensitive group
X61 303
X12 102
X110 607
MX158 704
X125 109
X1196 202
X193 102
X12 104
X61 301
MX158 702
X110 603
X125 110
X196 201
X193 101
JAK2
STAT3
STAT5
B-actin
B
JAK2
STAT3
STAT5
Relative JAK2 protein expression (JAK2/b-actin)
Relative STAT3 protein expression (STAT3/b-actin)
Relative STAT5 protein expression (STAT5/b-actin)
**
*
PTX sensitive
PTX resistance
C
PTX treated
PTX treated
Vehicle treated
**
****
D
Vehicle treated
Vehicle treated
PTX treated
***

Figure 3. The protein expression levels associated with the JAK-STAT pathway are upregulated in tumors of the paclitaxel-resistant group. Comparison of the protein expression levels of JAK2, STAT3, and STAT5 in the paclitaxel-resistant and -sensitive groups based on transcriptome data. (A) Western blot analysis data. (B-D) Comparative analysis of the protein expression levels of JAK2, STAT3, and STAT5 between the paclitaxel-sensitive and -resistant groups by quantification of Western blot data. Data were expressed as mean ± standard deviation (SD). Each experiment was performed in triplicate. * $p \leq 0.05$; ** $p \leq 0.01$; *** $p \leq 0.001$; **** $p \leq 0.0001$ (Mann-Whitney t-test). Quantification was performed using ImageJ software.

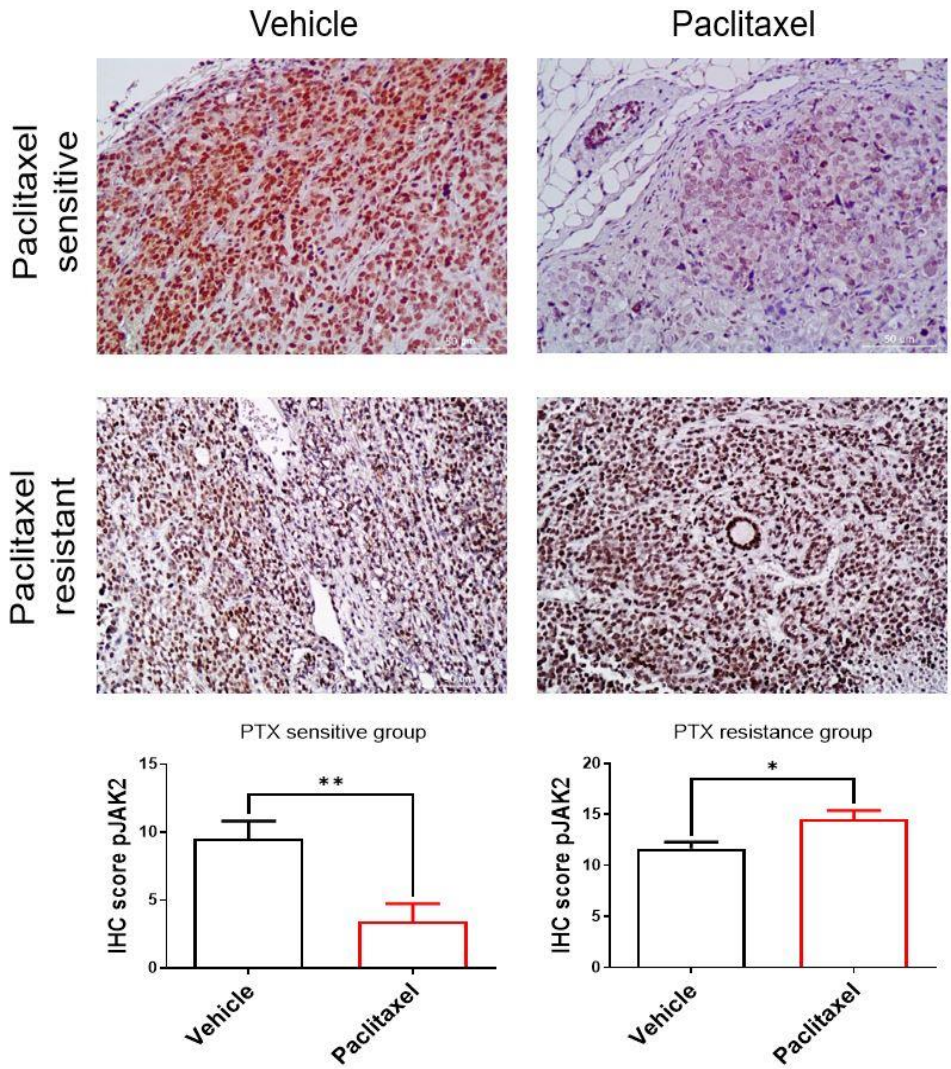

Figure 4. The activity of JAK2 is increased in paclitaxel resistance tumors.

Paraffin-embedded tissue microarray sections were formed through immunohistochemistry with anti-pJAK2 Ab. Representative photomicrographs of paclitaxel-sensitive or -resistant tumor tissue groups treated with vehicle or paclitaxel. Graphs represent quantification

immunostaining of pJAK2. * $p \leq 0.05$; ** $p \leq 0.01$ (Mann-Whitney t-test). Quantitative analysis was performed by IHC scoring by multiplying the stained area by the intensity.

Expression of JAK2, STAT3 and STAT5 in breast cancer cell lines

To investigate the mechanism of paclitaxel resistance by the upregulation of the JAK-STAT pathway, the JAK2, STAT3, and STAT5 genes and protein expression levels were analyzed via their mRNA and protein expression levels in 11 breast cancer cell lines. (MCF-7, ZR-75-1, SK-BR3, BT474, MDA-MB453, BT20, MDAMB231, MDA-MB468, HS578T, HCC38, and HCC70). The activation of the JAK-STAT pathway was confirmed by the expression levels of their activation forms, pSTAT3 and pSTAT5, by Western blotting. As a result, the gene (Figure 6B-6D) and protein (Figure 6A) expression levels of JAK2, STAT3, and STAT5 in each of the 11 breast cancer cell lines were varied. Based on qPCR and Western blot analyses, BT20, MDA-MB231, MDA-MB468, HCC38, and HCC70 TNBC cell lines, which were more expressed in either mRNA or protein levels than HS578T cells, were selected for further study.

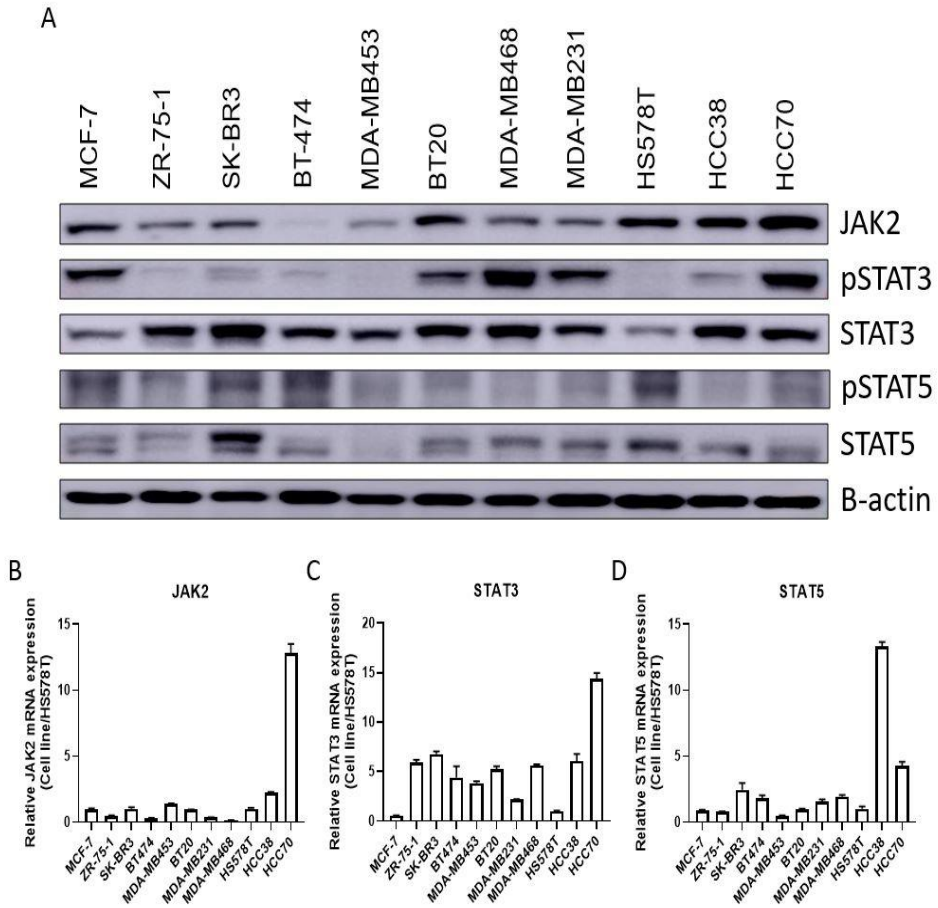

Figure 5. Tendency of mRNA and protein expression levels of JAK2, STAT3 and STAT5 in 11 breast cancer cell lines. (A) Using the 11 breast cancer cell lines, the protein expression levels of JAK2, STAT3, and STAT5, and their activation forms pSTAT3 and pSTAT5 were confirmed by Western blot (B–D). The gene expression levels of JAK2, STAT3, and STAT5 in 11 breast cancer cell lines were confirmed by qPCR. The gene expression levels of JAK2, STAT3, and STAT5 were normalized based on

the values of HS578T cells with the lowest gene expression levels ΔCt among the 11 breast cancer cell lines. Each experiment was performed in triplicate.

Mono-drug effects of paclitaxel and ruxolitinib on TNBC cell lines

The IC50 for each drug was measured to determine which concentrations of paclitaxel and ruxolitinib effectively inhibited cell proliferation in the selected five TNBC cell lines. Therefore, after treatment with paclitaxel or ruxolitinib from 0 to 1000nM for 72 h in five TNBC cell lines, cell viability was measured via an MTT assay. As a result, paclitaxel and ruxolitinib inhibited cell proliferation in a dose-dependent manner, although ruxolitinib effectively inhibited cell proliferation at higher concentrations than paclitaxel (Figure 7A and 7B). In detail, the paclitaxel IC50 values were: BT20, 5.5nM; HCC38, 11.0nM; HCC70, 7.2nM; MDAMB231, 12.2nM; MDA-MB468, 4.4nM. For ruxolitinib, the IC50 values were: BT20, 329.4nM; HCC38, 812.8nM; HCC70, 130.9nM; MDA-MB231, 412.0nM; MDA-MB468, 390.9nM (Table 2).

Table 2. IC50 of the paclitaxel or ruxolitinib only treated in five TNBC cell lines

Cancer cell lines	Drug	IC_{50} (nM)
BT20	Paclitaxel	5.5
	Ruxolitinib	329.4
HCC38	Paclitaxel	11.0
	Ruxolitinib	812.8
HCC70	Paclitaxel	7.2
	Ruxolitinib	130.9
MDA-MB231	Paclitaxel	12.2
	Ruxolitinib	412.0
MDA-MB468	Paclitaxel	4.4
	Ruxolitinib	390.9

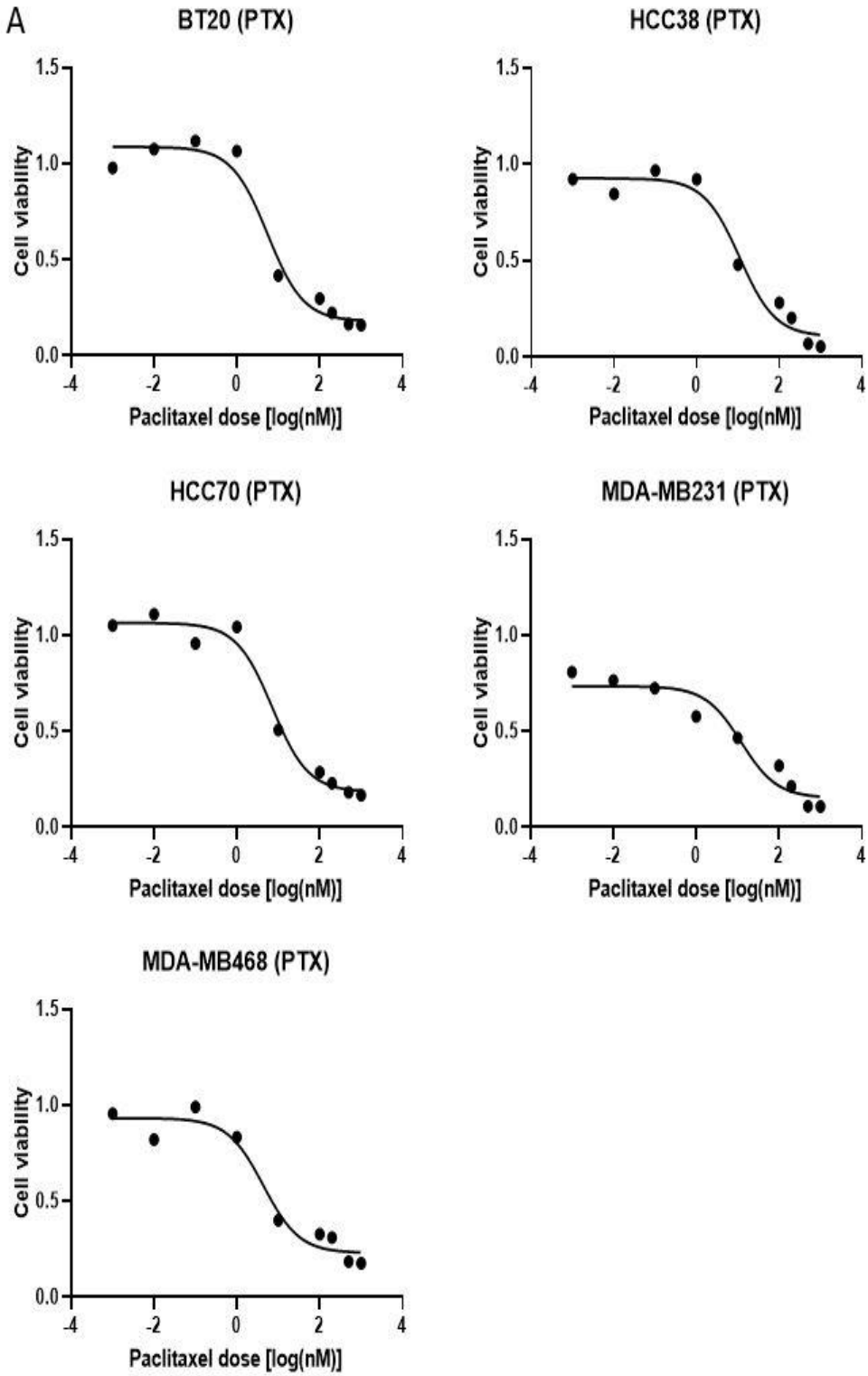
A
BT20 (PTX)
HCC38 (PTX)
HCC70 (PTX)
MDA-MB231 (PTX)
MDA-MB468 (PTX)
Cell viability
Paclitaxel dose [log(nM)]
1.5
1.0
0.5
0.0
-4
-2
0
2
4

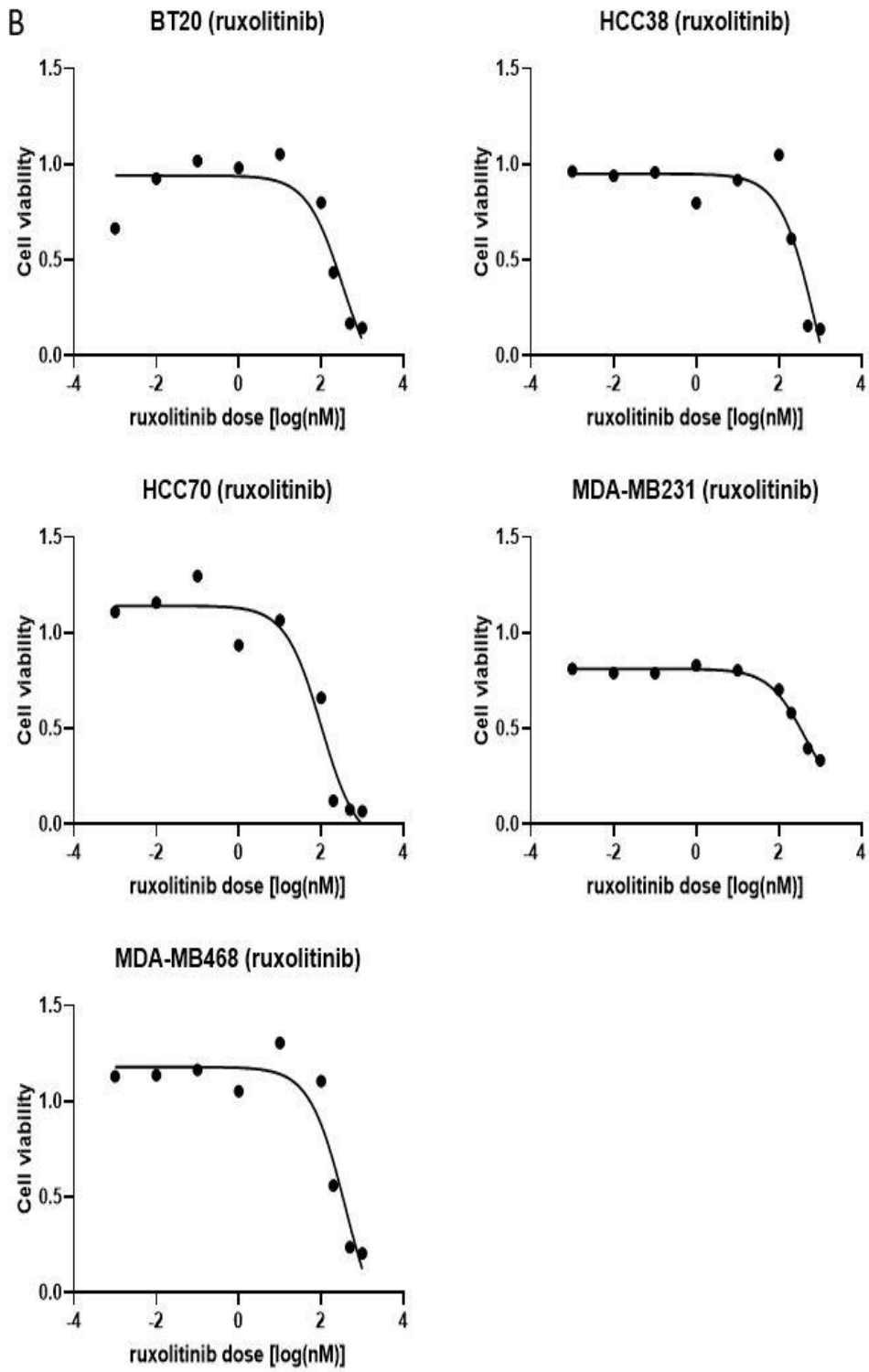
B
BT20 (ruxolitinib)
HCC38 (ruxolitinib)
HCC70 (ruxolitinib)
MDA-MB231 (ruxolitinib)
MDA-MB468 (ruxolitinib)
Cell viability
ruxolitinib dose [log(nM)]
1.5
1.0
0.5
0.0
-4
-2
0
2
4

Figure 6. The effect of paclitaxel or ruxolitinib cell proliferation on five TNBC cell lines *in-vitro*. In five TNBC cell lines, the effective concentration of the inhibition of cell proliferation when treated with paclitaxel or ruxolitinib. Each cell line's IC50 was measured via MTT assay. (A) Cell viability when treated with paclitaxel in five TNBC cell lines. (B) Cell viability when treated with ruxolitinib in five TNBC cell lines. Each experiment was performed in triplicate.

Ruxolitinib (JAKAVI) synergistic effect with paclitaxel in five TNBC cell lines.

Based on previous results, it was inferred that resistance to paclitaxel was associated with the upregulated JAK-STAT pathway. Therefore, the recovery of paclitaxel sensitivity when combined with ruxolitinib, a representative JAK1 and JAK2 inhibitor, in five TNBC cell lines was investigated. Ruxolitinib (JAKAVI) is a drug that is approved by the US FDA and is widely used to treat V617F leukemia [24-27]. In short, Ruxolitinib acts as an insulator as a JAK1 and JAK2 inhibitor, blocking signaling cascade by inhibiting the phosphorylation of JAK1 and JAK2 located in the cytoplasm cytokine or growth factor receptors. [37]

The IC50 of the paclitaxel- and ruxolitinib-only treatments, and the paclitaxel and ruxolitinib combination treatment in five TNBC cell lines were investigated. Each treatment was administered for 72h, then a cell viability assay was performed via an MTT assay. The synergy effects on two drugs were measured by referring to previous studies. [38, 39] The drug interaction score (FIC) for each combination was calculated by dividing the observed IC50 with the expected IC50. In short, the average IC50 value of

each drug is the expected IC50 and actually experimented the IC50 value of combination drugs is the expected IC50. FIC values are 1 for Loewe-additive pairs, and lower or higher than 1 for synergistic or antagonistic pairs. [38] As a result, all five TNBC cell lines showed a synergy effect when ruxolitinib and paclitaxel were treated simultaneously (Figure 7).

Consequently, the blocking of the JAK-STAT pathway by ruxolitinib was affect to paclitaxel sensitivity.

Table 3. IC50 of the paclitaxel- and ruxolitinib-only treatments and the paclitaxel and ruxolitinib combination treatment in five TNBC cell lines

Cancer cell lines	Drug	IC_{50} (nM)
BT20	Paclitaxel	7.21
	Combination	18.36
	Ruxolitinib	220.90
HCC38	Paclitaxel	18.08
	Combination	12.91
	Ruxolitinib	190.7
HCC70	Paclitaxel	8.60
	Combination	11.00
	Ruxolitinib	37.62
MDA-MB231	Paclitaxel	11.95
	Combination	47.63
	Ruxolitinib	258.7

Cancer cell lines	Drug	IC_{50} (nM)
MDA-MB468	Paclitaxel	40.55
	Combination	12.02
	Ruxolitinib	203.90

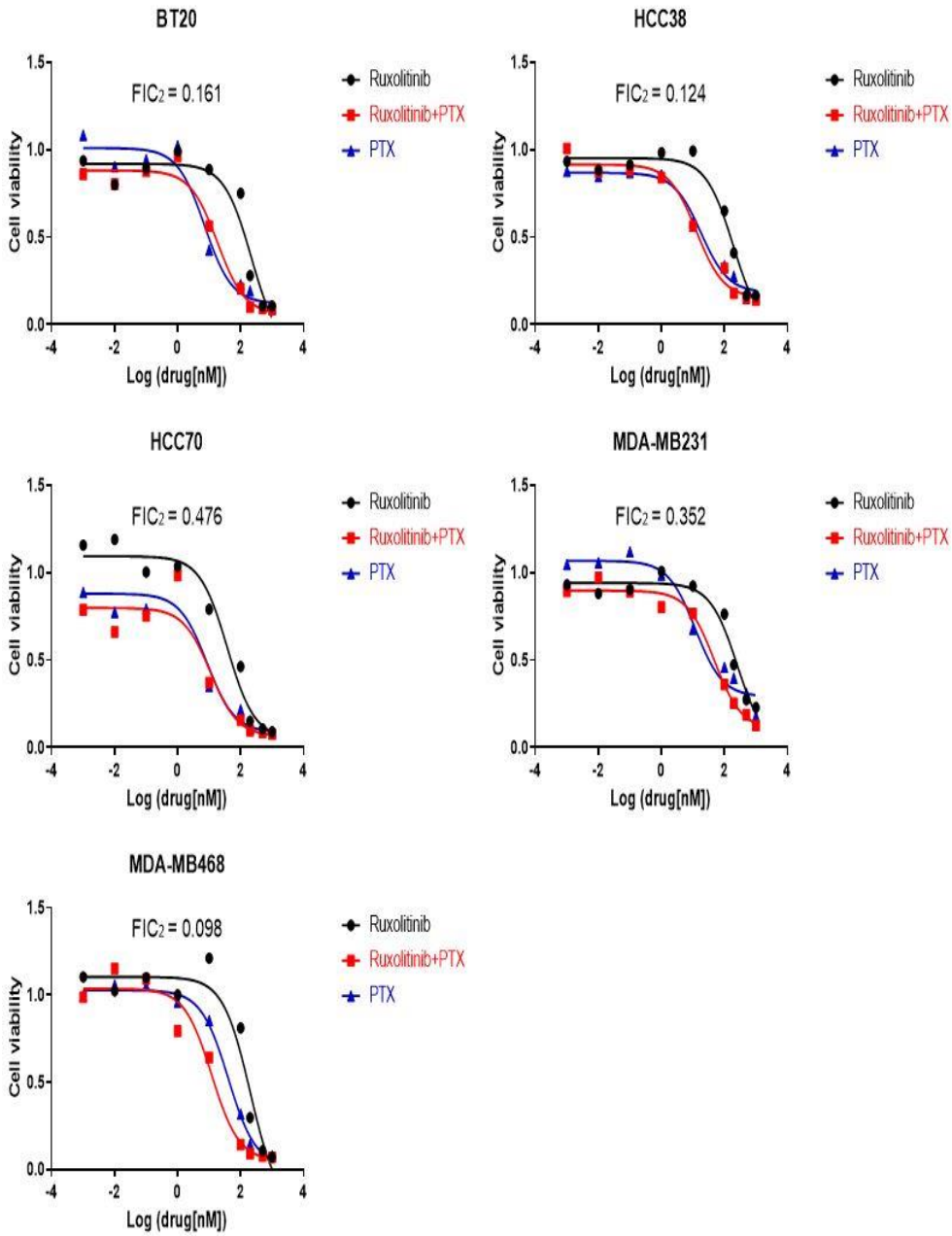

Figure 7. Synergistic effect of the paclitaxel and ruxolitinib combination treatment on five TNBC cell lines *in-vitro*. In five TNBC cell lines, a

synergistic effect occurred when paclitaxel and ruxolitinib were simultaneously administered. In detail, the FIC2 values were: BT20, 0.161; HCC38, 0.124; HCC70, 0.476; MDA-MB231, 0.352; and MDA-MB468, 0.098. Each experiment was performed in triplicate.

Ruxolitinib effectively inhibits JAK-STAT pathway in four TNBC cell lines

Whether ruxolitinib inhibited the JAK-STAT signaling pathway effectively in the TNBC cell lines was analyzed. Ruxolitinib was treated with increasing concentration from 0 to 1000nM for 24h, then proteins were extracted from four TNBC cell lines. The protein expression levels of JAK2, STAT3, and STAT5, as well as their active forms pJAK2, pSTAT3, and pSTAT5, were analyzed by Western blotting. Although slightly different for each cell line, the protein expressions of total JAK2, STAT3, and STAT5 decreased in all TNBC cell lines depending on the concentration of ruxolitinib (Figure 8). In addition, the expression levels of these active forms, pJAK2, pSTAT3, and pSTAT5, were also reduced depending on the concentration of ruxolitinib. Therefore, ruxolitinib effectively inhibited activation of the JAK-STAT signaling pathways.

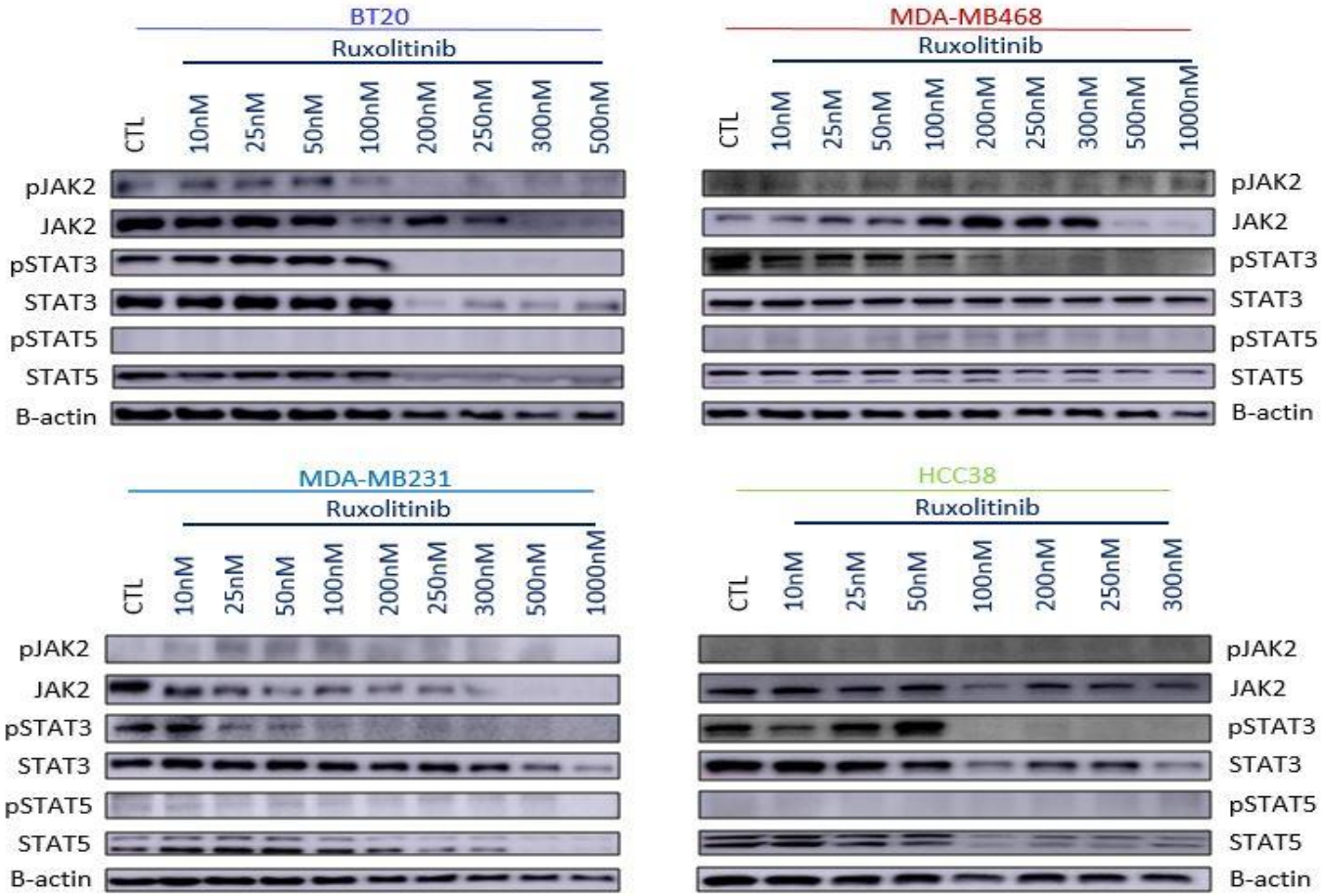
BT20
Ruxolitinib
CTL
10nM
25nM
50nM
100nM
200nM
250nM
300nM
500nM
pJAK2
JAK2
pSTAT3
STAT3
pSTAT5
STAT5
B-actin
MDA-MB468
Ruxolitinib
CTL
10nM
25nM
50nM
100nM
200nM
250nM
300nM
500nM
1000nM
pJAK2
JAK2
pSTAT3
STAT3
pSTAT5
STAT5
B-actin
MDA-MB231
Ruxolitinib
CTL
10nM
25nM
50nM
100nM
200nM
250nM
300nM
500nM
1000nM
pJAK2
JAK2
pSTAT3
STAT3
pSTAT5
STAT5
B-actin
HCC38
Ruxolitinib
CTL
10nM
25nM
50nM
100nM
200nM
250nM
300nM
pJAK2
JAK2
pSTAT3
STAT3
pSTAT5
STAT5
B-actin

Figure 8. Ruxolitinib effectively inhibits the JAK-STAT pathway in four TNBC cell lines *in-vitro*. Ruxolitinib was administered at increasing concentrations from 0 to 1000nM for 24h in four TNBC cell lines. The activation of JAK2, STAT3, and STAT5 decreased in a concentration-dependent manner with the concentrations of ruxolitinib in four TNBC cell lines. these data were analyzed with three repeats.

Inhibition of JAK2 is associated with improved response to paclitaxel.

A synergistic effect was observed when ruxolitinib and paclitaxel were administered simultaneously. In addition, to determine whether the recovery of paclitaxel sensitivity by paclitaxel and ruxolitinib combination treatment is due to the inhibition of JAK2 in TNBC cell lines. The IC50 of paclitaxel was analyzed in four TNBC cell lines after the inactivation of JAK2 using JAK2 siRNA. The inhibition of JAK2 by JAK2 siRNA was confirmed by Western blot (Figure 9A), and IC50 measurements were then performed. When paclitaxel was administered for 72h and compared with NTC, three TNBC cell lines (BT20, HCC38, and MDA-MB231) knocked down JAK2, except the MDA-MB468 cell line, showing dramatically reduced IC50 for paclitaxel (Figure 9B and Table 3). Therefore, it was confirmed that the JAK2 signaling pathway affects sensitivity to paclitaxel.

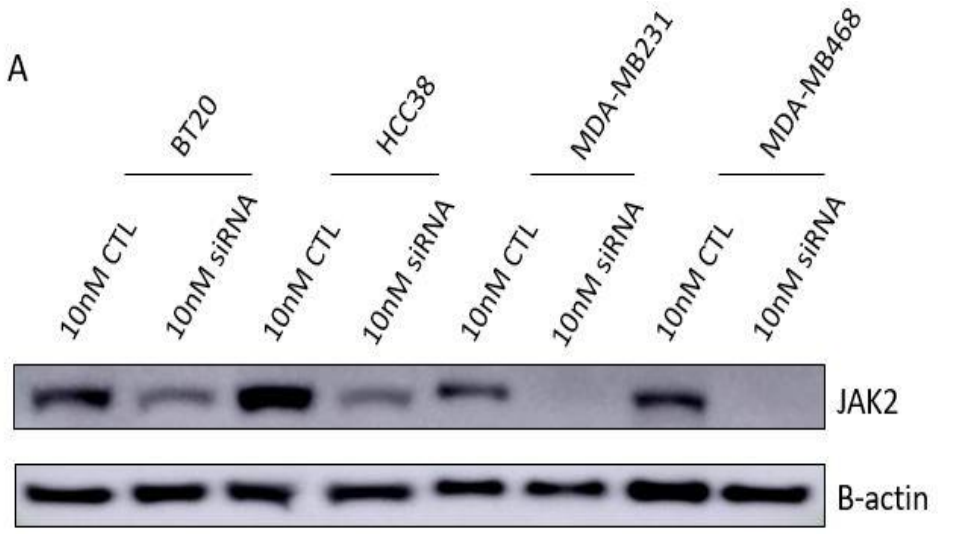
A
BT20
HCC38
MDA-MB231
MDA-MB468
10nM CTL
10nM siRNA
10nM CTL
10nM siRNA
10nM CTL
10nM siRNA
10nM CTL
10nM siRNA
JAK2
B-actin

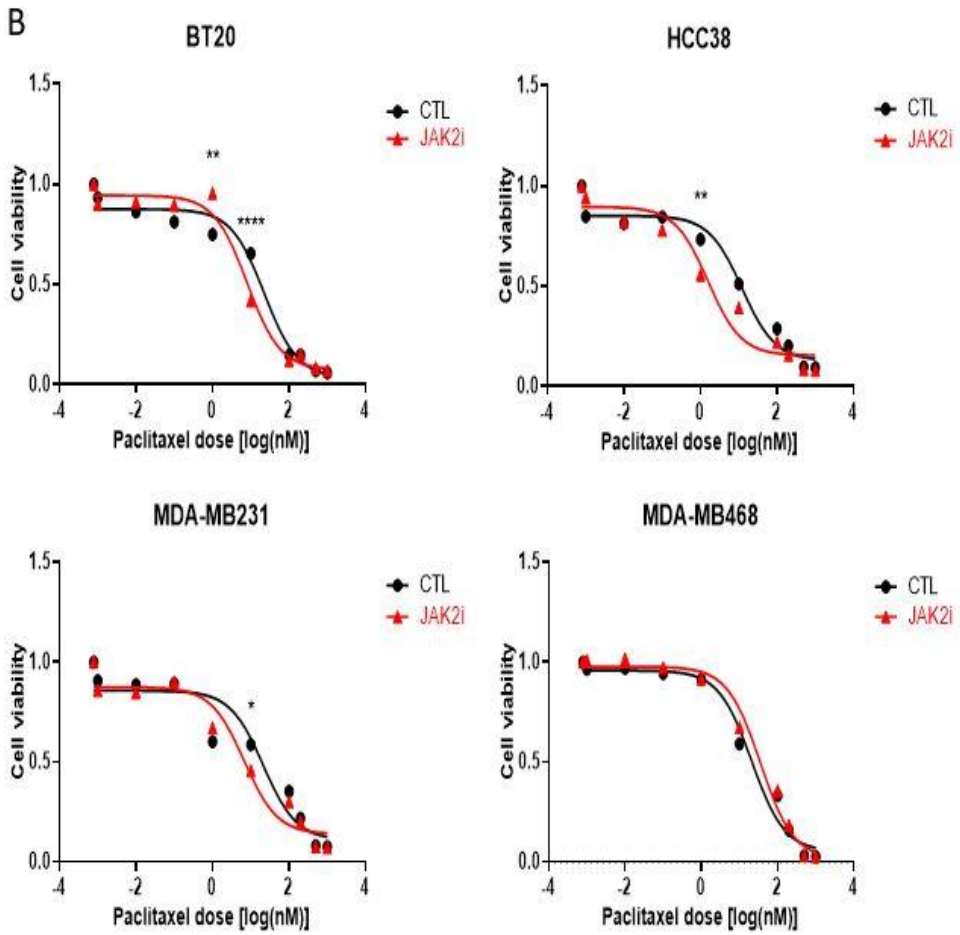
B
BT20
HCC38
MDA-MB231
MDA-MB468
CTL
JAK2i
Cell viability
Paclitaxel dose [log(nM)]
**
****
**
*

Figure 9. Response to paclitaxel improved JAK2i TNBC cell lines *in-vitro*.

Paclitaxel inhibited four TNBC cell lines' survival in a dose-dependent manner. Control and JAK2 transfection of four TNBC cells were treated with paclitaxel for 72 h. IC50 was measured using MTT arrays, and data were expressed as mean ± standard deviation (SD). Each experiment was performed in triplicate. * $p \leq 0.05$; ** $p \leq 0.01$; *** $p \leq 0.001$; **** $p \leq 0.0001$ (multiple t-test).

Table 4. IC50 of Paclitaxel in silencing siCONTROL (NTC) and siJAK2 (JAK2i) in four TNBC cell lines.

Cancer cell lines	Drug	IC_{50} (nM)
BT20 (NTC)	Paclitaxel	22.62
BT20 (JAK2i)	Paclitaxel	8.01
HCC38 (NTC)	Paclitaxel	12.17
HCC38 (JAK2i)	Paclitaxel	1.579
MDA-MB231 (NTC)	Paclitaxel	21.31
MDA-MB231 (JAK2i)	Paclitaxel	6.71
MDA-MB468 (NTC)	Paclitaxel	20.94
MDA-MB468 (JAK2i)	Paclitaxel	35.43

Upregulated cell cycle-related genes in the micro-environment in paclitaxel resistance tumors.

The JAK-STAT signaling pathway activity affects not only the tumors but also their microenvironments. Previous studies have shown that cancer-associated fibroblasts (CAFs) promote cancer stem cell renewal and stem cell proliferation capacity through high levels of IL-6 and CCL2 upon STAT3 activation [40] and cancer-associated adipocytes promoted radiation therapy resistance via the upregulation of IL-6 expression in breast cancer [41]. Therefore, we analyzed the expression changes of mouse genes between the paclitaxel-resistance and -sensitive group in transcriptome data.

By utilizing DAVID Functional Annotation Bioinformatics Microarray Analysis (https://david.ncifcrf.gov/), the pathways that were activated using the gene set of mice with increased expression in the paclitaxel-resistant group were analyzed. As a result, it was found that the cell cycle pathway was followed by DNA replication, oocyte meiosis, and small cell lung cancer. These were activated in the microenvironments around the tumors of the paclitaxel-resistant group, and the difference was statistically significant.

(Table 5) Therefore, it was found that cell proliferation is upregulated in the microenvironments around paclitaxel-resistant tumors

Table 5. Upregulated cell cycle-related genes in tumor microenvironments of the paclitaxel-resistant group.

Pathway	Count	PValue	Genes
Cell cycle	32	1.23E-21	E2F2, DBF4, TTK, PKMYT1, CHEK1, PTTG1, TGFB2, CCNE2, CCNE1, CDC45, MCM7, BUB1, CCNA2, ORC1, CDC7, CDC6, CDK1, RBL1, CDC20, ESPL1, MCM2, CDC25C, MCM3, MCM4, MCM5, MCM6, CCNB1, CCND1, MAD2L1, CCNB2, PLK1, BUB1B
DNA replication	12	1.46E-09	PRIM1, RFC5, DNA2, MCM7, LIG1, POLE, POLA1, MCM2, MCM3, MCM4, MCM5, MCM6
Oocyte meiosis	16	4.36E-07	CDK1, SGOL1, PKMYT1, ESPL1, AURKA, CDC20, PTTG1, CDC25C, CCNE2, CCNB1, CCNE1, CCNB2, MAD2L1, PLK1, BUB1, FBXO5
Small cell lung cancer	13	3.21E-06	E2F2, CKS1B, COL4A2, COL4A1, ITGA3, CCNE2, CCNE1, CCND1, LAMA4, ITGA6, CKS2, LAMC1, NOS2
Fanconi anemia pathway	10	9.67E-06	RAD51C, BLM, APITD1, FANCI, EME1, BRIP1, FANCA, BRCA1, FANCB, RAD51
PI3K-Akt signaling pathway	25	4.13E-05	EFNA1, ITGB3, CCNE2, CCNE1, GM15776, INSR, ANGPT2, IL6, COL4A2, IL2RA, FLT1, COL4A1, FLT4, NR4A1, ITGA3, EPHA2, BRCA1, KDR, VWF, VEGFC, CCND1, LAMA4, ITGA6, IFNB1, LAMC1
p53 signaling pathway	10	9.22E-05	CCNE2, CCNB1, CDK1, CCNE1, CCND1, CCNB2, RRM2, CHEK1, PIDD1, GTSE1
Pathways in cancer	25	2.59E-04	E2F2, CKS1B, BDKRB2, TGFB2, CCNE2, CCNE1, RASGRP3, NOS2, GM15776, BMP4, TCF7, IL6, COL4A2, COL4A1, ITGA3, BIRC5, MECOM, FZD6, RAD51, VEGFC, LAMA4, CCND1, ITGA6, CKS2, LAMC1
Toxoplasmosis	11	6.72E-04	LAMA4, CCR5, ITGA6, HSPA1A, IL12B, NOS2, LAMC1, HSPA1B, H2-DMA, H2-DMB2, TGFB2

ECM-receptor interaction	10	7.42E-04	VWF, COL4A2, LAMA4, COL4A1, ITGA6, NPNT, ITGA3, LAMC1, ITGB3, HMMR
Cytokine-cytokine receptor interaction	17	0.001185209	IL6, IL2RA, CCR1, CCL5, TNFSF18, TNFSF8, TGFB2, IL11, CXCL10, CCL12, CCR5, TNFSF13B, PPBP, IFNB1, CX3CR1, IL12B, IFNLR1
Pyrimidine metabolism	10	0.001851466	PRIM1, DCTD, TYMS, RRM2, POLE, POLA1, DCK, NT5E, TK1, DUT
Focal adhesion	15	0.001933073	PARVG, COL4A2, FLT1, COL4A1, FLT4, MYLPF, ITGA3, ITGB3, KDR, VWF, VEGFC, CCND1, LAMA4, ITGA6, LAMC1
Rheumatoid arthritis	9	0.001974306	CCL12, IL6, FLT1, TNFSF13B, CCL5, H2-DMA, H2-DMB2, TGFB2, IL11
African trypanosomiasis	6	0.002669321	HBA-A1, IL6, LAMA4, HBB-BS, IL12B, HBB-BT
Progesterone-mediated oocyte maturation	9	0.002874	CCNB1, CDK1, MAD2L1, CCNB2, PLK1, BUB1, PKMYT1, CDC25C, CCNA2
Cell adhesion molecules (CAMs)	12	0.005608879	F11R, MPZL1, ICOSL, ITGA6, CD34, ICAM2, CLDN5, ESAM, H2-DMA, PDCD1, H2-DMB2, CDH5
Homologous recombination	5	0.007179496	RAD51C, BLM, EME1, RAD54L, RAD51
Hematopoietic cell lineage	8	0.009440762	SIGLECH, IL6, IL2RA, ITGA6, CD34, ITGA3, ITGB3, IL11
Malaria	6	0.010507177	HBA-A1, CCL12, IL6, HBB-BS, HBB-BT, TGFB2
Measles	10	0.013782577	CCNE2, CCNE1, IL6, CCND1, IL2RA, IFNB1, TACR1, HSPA1A, IL12B, HSPA1B
Amoebiasis	9	0.016505573	COL4A2, IL6, LAMA4, COL4A1, SERPINB2, IL12B, NOS2, LAMC1, TGFB2
Rap1 signaling pathway	13	0.016667151	VEGFC, FLT1, RASGRP3, EFNA1, FLT4, RAPGEF4, ITGB3, ARAP3, ANGPT2, INSR, EPHA2, DOCK4, KDR
Chagas disease (American trypanosomiasis)	8	0.024952209	CCL12, IL6, IFNB1, IL12B, NOS2, BDKRB2, CCL5, TGFB2

Increased proliferation of fibroblast and endothelial cells in the micro-environment in the tumors of the paclitaxel-resistant group

To determine which cell proliferation increased around the tumors of the paclitaxel-resistant group, the IHC staining of paclitaxel-resistant and -sensitive tumors was analyzed using the KI-67 antibody, a cell proliferation marker. It was found that KI-67 expression increased in the tumors of the paclitaxel-resistant group compared to the tumors of the paclitaxel-sensitive group in the surrounding tumor cells, such as fibroblast (Figure 10A) and endothelial cells (Figure 10B). In addition, to identified whether they were actually fibroblast and endothelial cells, IHC staining was conducted using the α-SMA and CD31 antibody, a fibroblast marker and an endothelial cell marker.

Then, the number of KI-67 positive endothelial cells and fibroblasts in the tumors of both the paclitaxel-resistant and -sensitive group were counted to compare the number of KI-67 positive endothelial cells and fibroblasts in the tumors. As a result, in the tumors of the paclitaxel-resistant group, a greater number of KI-67 positive endothelial cells and

fibroblast were found compared to that of the paclitaxel-sensitive group, (Figure 10C). Consequently, tumors of the paclitaxel-resistant group upregulated the proliferation of fibroblast and endothelial cells *in-vivo*.

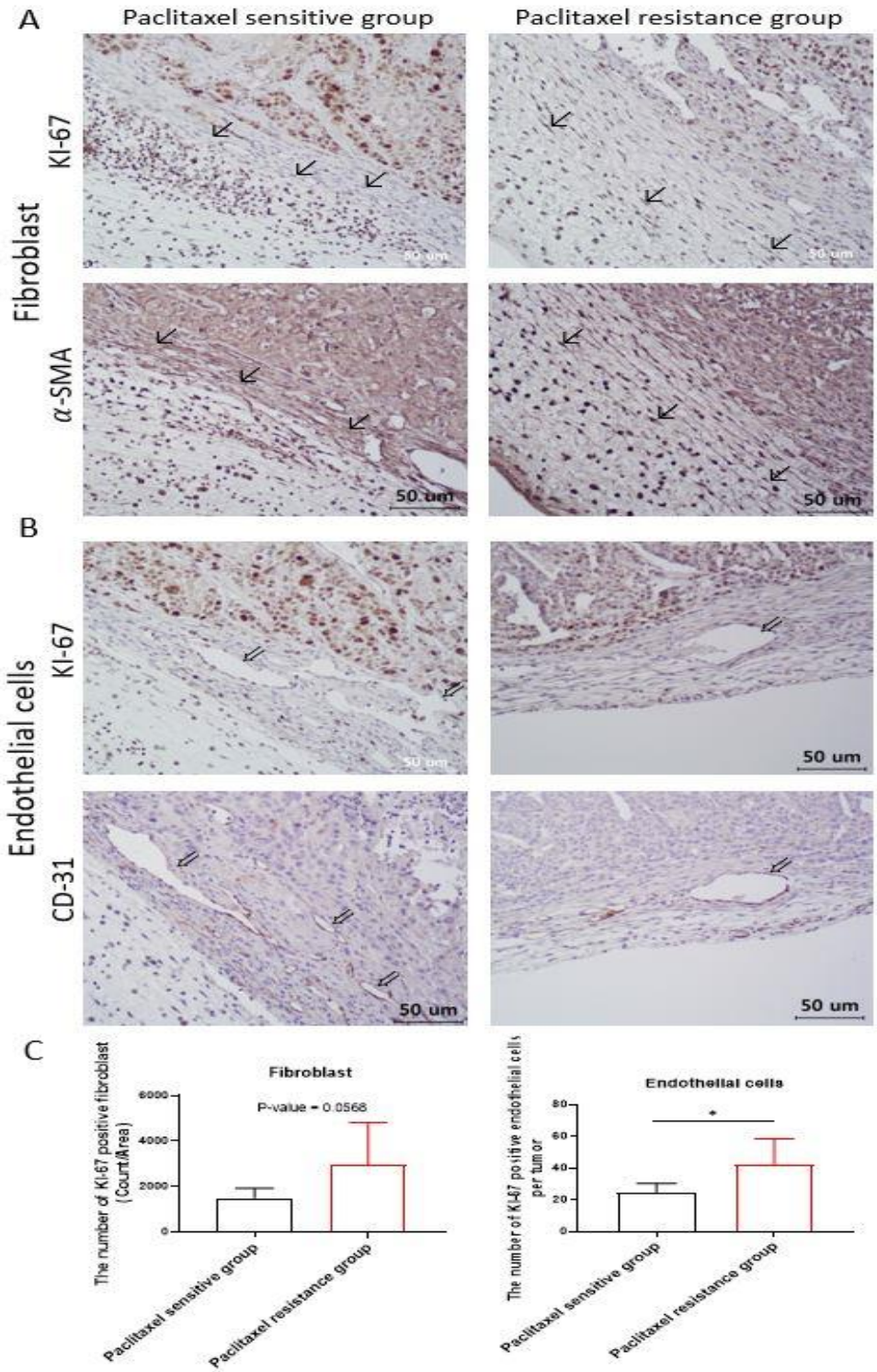
A
Paclitaxel sensitive group
Paclitaxel resistance group
Fibroblast
KI-67
α-SMA
50 um
B
Endothelial cells
KI-67
CD-31
50 um
C
Fibroblast
P-value = 0.0568
The number of KI-67 positive fibroblast (Count/Area)
6000
4000
2000
0
Paclitaxel sensitive group
Paclitaxel resistance group
Endothelial cells
*
The number of KI-67 positive endothelial cells per tumor
80
60
40
20
0
Paclitaxel sensitive group
Paclitaxel resistance group

Figure 10. The upregulated proliferation of endothelial cells and fibroblasts in tumors of the paclitaxel-resistant group. Paraffin-embedded tissue microarray sections were identified through IHC with anti-Ki67, α-SMA, CD31 antibody. (A) The black arrow indicates the fibroblasts in the tumor. (B) The black open arrow indicates the endothelial cells in the tumor. Representative photomicrographs of the paclitaxel-sensitive or -resistant group tumor tissues. (C) The differences in the number of KI-67 positive fibroblasts and endothelial cells between the paclitaxel-resistant and -sensitive tumors were counted in the tumor tissues and quantified. Data were expressed as mean ± standard deviation (SD). * $p \leq 0.05$ (Mann-Whitney t-test).

The decreased proliferation of fibroblasts in the inhibition of the JAK2 TNBC cell line conditioned media

To determine whether the JAK-STAT pathway activity affects the fibroblasts that comprise the micro-environment around the tumor, the effects of conditioned media (CM) extracted from JAK2 inhibited TNBC cell lines on the fibroblasts of mice proliferation were analyzed using an MTT assay. As a result, it was confirmed that proliferation decreased in fibroblasts incubated in CM extracted from JAK2-inhibited TNBC cell lines, and the difference was statistically significant (Figure 11). Therefore, it confirmed that the activation of the JAK-STAT signaling pathway affects the proliferation of fibroblasts comprising the micro-environment around the tumors.

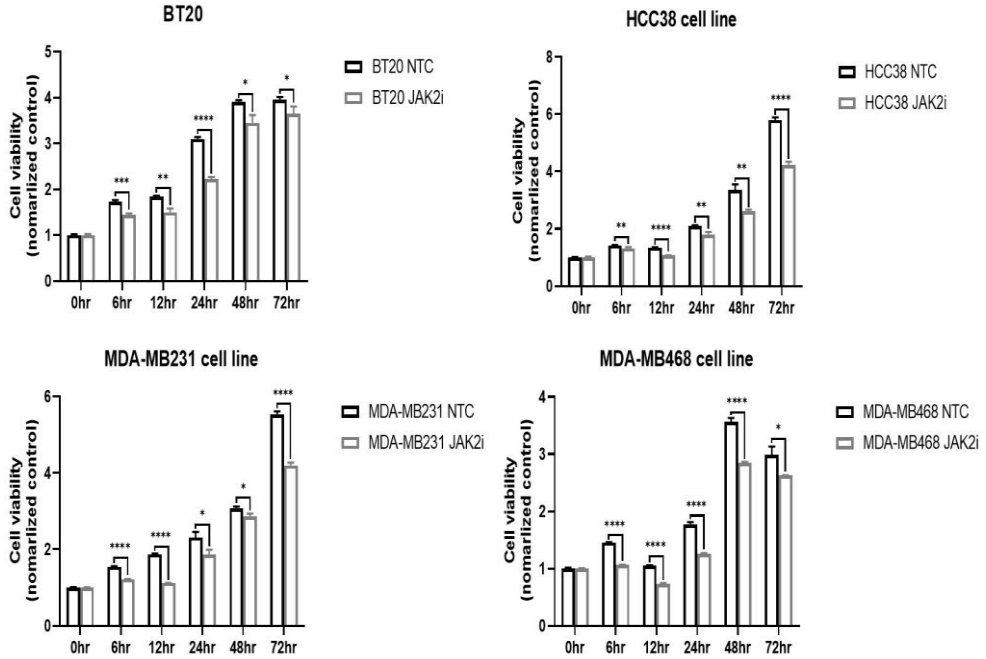

Figure 11. Decreased proliferation of fibroblasts incubated in conditioned media extracted from JAK2 inhibited TNBC cell lines. The proliferation of mouse fibroblasts treated with NTC or JAK2i CM was compared. The inhibition of TNBC cell lines were placed in CM for 72 h. Mouse fibroblast proliferation was measured using MTT arrays. Data were expressed as mean ± standard deviation (SD). Each experiment was performed in triplicate. * $p \leq 0.05$; ** $p \leq 0.01$; *** $p \leq 0.001$; **** $p \leq 0.0001$ (Multiple t-test).

Discussion

Paclitaxel is a common chemotherapeutic agent for breast cancer treatment, but the anti-tumor activity of paclitaxel is limited by resistance, which is naturally acquired after long-term exposure. One of the challenges in treating breast cancer is chemotherapy resistance. In this study, we investigated how the activation of the JAK-STAT pathway affects paclitaxel resistance in TNBC. Paclitaxel was administered for 4 weeks to seven PDX models of TNBC-derived tissues. Then, reactivity with the paclitaxel-resistant and -sensitive group was established via differences in the rate of tumor size reduction caused by paclitaxel. RNA transcriptome analysis showed that the expression levels of genes related to the JAK-STAT pathway increased in paclitaxel-resistant tumors. Therefore, we hypothesized that paclitaxel resistance in TNBC may be related to the activity of the JAK-STAT pathway. Additionally, western blot assay confirmed that paclitaxel-resistant TNBC tumors upregulated the protein expression levels of JAK2, STAT3, and STAT5 as well as increased the

activation of the JAK-STAT pathway through the upregulated protein expression of pJAK2.

To investigate the mechanism of paclitaxel resistance by the upregulation of the JAK-STAT pathway, various experiments were performed on TNBC cell lines. The mRNA and protein expression levels of the JAK2, STAT3, and STAT5 were analyzed in 11 breast cancer cell lines. Of the 11 breast cancer cell lines, five TNBC cell lines were selected that had high expression and activity of JAK-STAT signaling pathway. In addition, it was confirmed that the anti-tumor function of paclitaxel increased when JAK2 was blocked through ruxolitinib, JAK1, and JAK2 inhibitors or siRNA. As a result, the JAK-STAT pathway activity was found to be correlated with paclitaxel resistance. Consequently, the JAK-STAT signaling pathway was found to affect sensitivity to paclitaxel.

To overcome chemotherapy resistance in breast cancer, various treatment methods have been introduced, such as the use of new potent anti-cancer reagents and combination chemotherapy with targeted agents. Previous studies have reported several methods for the treatment of paclitaxel-resistant cancers [42-44]. This study demonstrates that in

TNBC, the chemoresistance of paclitaxel is associated with the upregulation of JAK-STAT pathway activity.

The JAK-STAT pathway affects many cancers. In recent studies, the activation of JAK-STAT signaling enhanced the proliferation of cancer stem cells (CSCs), such as side populations, [45] cancer cell migration, [46] and tumor progression. [47] In breast cancer, carcinogenicity is caused by the activity of STAT3 [48], and lasting STAT3 activation in about 70% of breast cancers [49] Overall, STAT3 activation is found, regardless of subtypes, in breast cancer, but is most associated with TNBC. [50, 51] A recent study showed that advanced breast tumor progression is due to constantly active STAT3 caused by exploited cancer cell proliferation, angiogenesis, and EMT. [52] Specifically, STAT3 can upregulate genes promoting angiogenesis (VEGF), anti-apoptosis (such as bcl-xl and mcl1), invasion (MMP1), and proliferation (cyclinD1)-related proteins. [53] STAT5 promotes differentiation of the mammary gland and upregulates anti-apoptosis genes. [54] More frequently in hormone responsive breast cancers, abiding activation of STAT5 has been confirmed. [50, 54] Additionally, mice experience progression in mammary tumors via the

constitutive upregulation of STAT5 activity [55]. A recent study revealed that the constitutive JAK2 activation caused by the V617F mutation occurs due to the upregulation of STAT5 activity, leading to increased tumor growth and the blocking of cancer cell death in breast cancer.[56]

Inhibition of the JAK-STAT signaling pathway can potentially promote the anti-tumor activity of paclitaxel in TNBC. Although the mechanism by which the JAK-STAT pathway affects paclitaxel resistance is currently unknown, the results of the present study suggest that the inhibition of JAK-STAT signaling pathway may increase sensitivity to paclitaxel via the regulation of tumor micro-environments, such as cancer-associated fibroblasts (CAFs) and endothelial cells. Previous studies have shown that cancer-associated fibroblasts (CAFs) promote cancer stem cell renewal and mammosphere forming capacity through promoted JAK-STAT signaling [40] and cancer-associated adipocytes promoted radiation therapy resistance via the upregulation of IL-6 expression in breast cancer [41]. In breast cancer, it has been reported that CAFs are associated with resistance to chemotherapeutic drugs, such as paclitaxel. [57]

This study has some important limitations. First, the number of TNBC PDX models used in this experiment is limited. Seven TNBC PDX models were applied and a paclitaxel-sensitive and -resistant group were established according to the relative rate of reduction of tumor size after paclitaxel treatment. Then, RNA transcriptome was used to select genes with differences in gene expression between these two groups. Therefore, there may be enough error in the selection of genes related to paclitaxel resistance, so it is necessary to confirm whether this tendency is shown for other TNBC PDX models with paclitaxel resistance. Second, there is a lack of comparative data in other breast cancer subtypes, such as luminal or HER2+. A recent study showed that the activation of JAK2 and STAT3 is associated with resistance to tamoxifen in luminal subtype breast cancer. [58] Therefore, in addition to TNBC, other subtypes may cause chemotherapy resistance through the activation of the JAK-STAT pathway. Further studies related to the JAK-STAT pathway should be conducted on other subtypes of breast cancer. In this study, the paclitaxel-resistant and -sensitive groups were established via in vivo experiments using the TNBC PDX models. However, in vitro experiments were performed using general

TNBC cell lines. Therefore, it is necessary to establish stabilized paclitaxel-resistant breast cancer cell lines to confirm the experiments associated with paclitaxel resistance, and that they have the results and reproducibility tested in this study. There is currently a limit to our ability to fully understand how the activation of the JAK-STAT pathway acts on paclitaxel resistance associated with tumor microenvironments. Therefore, further studies are needed to elucidate this mechanism.

References

1. Jung, K.W., et al., *Cancer Statistics in Korea: Incidence, Mortality, Survival, and Prevalence in 2016.* Cancer Res Treat, 2019. **51**(2): p. 417-430.

2. Criscitiello, C., et al., *Understanding the biology of triple-negative breast cancer.* Annals of Oncology, 2012. **23**: p. 13-18.

3. Shao, F.Y., H. Sun, and C.X. Deng, *Potential therapeutic targets of triple-negative breast cancer based on its intrinsic subtype.* Oncotarget, 2017. **8**(42): p. 73329-73344.

4. Jhan, J.R. and E.R. Andrechek, *Triple-negative breast cancer and the potential for targeted therapy.* Pharmacogenomics, 2017. **18**(17): p. 1595-1609.

5. Taxman, D.J., et al., *Transcriptional profiling of targets for combination therapy of lung carcinoma with paclitaxel and mitogen-activated protein/extracellular signal-regulated kinase kinase inhibitor.* Cancer Res, 2003. **63**(16): p. 5095-104.

6. Blagosklonny, M.V. and T. Fojo, *Molecular effects of paclitaxel: Myths and reality (a critical review).* International Journal of Cancer, 1999. **83**(2): p. 151-156.

7. Jordan, M.A. and L. Wilson, *Microtubules as a target for anticancer drugs.* Nature Reviews Cancer, 2004. **4**(4): p. 253-265.

8. Zasadil, L.M., et al., *Cytotoxicity of Paclitaxel in Breast Cancer Is due to Chromosome Missegregation on Multipolar Spindles.* Science Translational Medicine, 2014. **6**(229).

9. Westerhoff, H.V., A. Riethorst, and A.P.M. Jongsma, *Relating*

multidrug resistance phenotypes to the kinetic properties of their drug-efflux pumps. European Journal of Biochemistry, 2000. **267**(17): p. 5355-5368.

10. Kadoyama, K., et al., *Hypersensitivity reactions to anticancer agents: data mining of the public version of the FDA adverse event reporting system, AERS.* J Exp Clin Cancer Res, 2011. **30**: p. 93.

11. Tanimukai, H., et al., *Paclitaxel induces neurotoxicity through endoplasmic reticulum stress.* Biochemical and Biophysical Research Communications, 2013. **437**(1): p. 151-155.

12. Symmans, W.F., *Breast cancer response to paclitaxel in vivo.* Drug Resistance Updates, 2001. **4**(5): p. 297-302.

13. Bournazou, E. and J. Bromberg, *Targeting the tumor microenvironment: JAK-STAT3 signaling.* JAKSTAT, 2013. **2**(2):

p. e23828.

14. O'Shea, J.J., et al., *The JAK-STAT Pathway: Impact on Human Disease and Therapeutic Intervention.* Annual Review of Medicine, Vol 66, 2015. **66**: p. 311-328.

15. Liongue, C., R. Sertori, and A.C. Ward, *Evolution of Cytokine Receptor Signaling.* Journal of Immunology, 2016. **197**(1): p. 11-18.

16. Britschgi, A., et al., *JAK2/STAT5 Inhibition Circumvents Resistance to PI3K/mTOR Blockade: A Rationale for Cotargeting These Pathways in Metastatic Breast Cancer.* Cancer Cell, 2012. **22**(6): p. 796-811.

17. Creamer, B.A., et al., *Stat5 promotes survival of mammary epithelial cells through transcriptional activation of a distinct promoter in Akt1.* Mol Cell Biol, 2010. **30**(12): p. 2957-70.

18. Hosford, S.R. and T.W. Miller, *Clinical potential of novel therapeutic targets in breast cancer: CDK4/6, Src, JAK/STAT, PARP, HDAC, and PI3K/AKT/mTOR pathways.* Pharmgenomics Pers Med, 2014. **7**: p. 203-15.

19. Iavnilovitch, E., et al., *Deregulation of Stat5 expression and activation causes mammary tumors in transgenic mice.* Int J Cancer, 2004. **112**(4): p. 607-19.

20. Marotta, L.L., et al., *The JAK2/STAT3 signaling pathway is required for growth of CD44(+)CD24(-) stem cell-like breast cancer cells in human tumors.* J Clin Invest, 2011. **121**(7): p. 2723-35.

21. O'Shea, J.J., S.M. Holland, and L.M. Staudt, *JAKs and STATs in immunity, immunodeficiency, and cancer.* N Engl J Med, 2013. **368**(2): p. 161-70.

22. Ren, S.X., et al., *Loss of Stat5a delays mammary cancer progression in a mouse model.* Oncogene, 2002. **21**(27): p. 4335-4339.

23. Schmidt, J.W., et al., *Stat5 Regulates the Phosphatidylinositol 3-Kinase/Akt1 Pathway during Mammary Gland Development and Tumorigenesis.* Molecular and Cellular Biology, 2014. **34**(7): p. 1363-1377.

24. Quintas-Cardama, A. and S. Verstovsek, *Molecular pathways: Jak/STAT pathway: mutations, inhibitors, and resistance.* Clin Cancer Res, 2013. **19**(8): p. 1933-40.

25. Verstovsek, S., et al., *Long-term treatment with ruxolitinib for patients with myelofibrosis: 5-year update from the randomized, double-blind, placebo-controlled, phase 3 COMFORT-I trial.* J Hematol Oncol, 2017. **10**(1): p. 55.

26. Saenz, D.T., et al., *BET protein bromodomain inhibitor-based combinations are highly active against post-myeloproliferative neoplasm secondary AML cells.* Leukemia, 2017. **31**(3): p. 678-687.

27. Yu, H.A., et al., *A Phase 1/2 Trial of Ruxolitinib and Erlotinib in Patients with EGFR-Mutant Lung Adenocarcinomas with Acquired Resistance to Erlotinib.* J Thorac Oncol, 2017. **12**(1): p. 102-109.

28. Hurwitz, H.I., et al., *Randomized, Double-Blind, Phase II Study of Ruxolitinib or Placebo in Combination With Capecitabine in Patients With Metastatic Pancreatic Cancer for Whom Therapy With Gemcitabine Has Failed.* Journal of Clinical Oncology, 2015. **33**(34): p. 4039-+.

29. Ju, W., et al., *Augmented efficacy of brentuximab vedotin combined with ruxolitinib and/or Navitoclax in a murine model of human*

Hodgkin's lymphoma. Proceedings of the National Academy of Sciences of the United States of America, 2016. **113**(6): p. 1624-1629.

30. Dobin, A., et al., *STAR: ultrafast universal RNA-seq aligner.* Bioinformatics, 2013. **29**(1): p. 15-21.

31. Anders, S., P.T. Pyl, and W. Huber, *HTSeq-a Python framework to work with high-throughput sequencing data.* Bioinformatics, 2015. **31**(2): p. 166-169.

32. Robinson, M.D., D.J. McCarthy, and G.K. Smyth, *edgeR: a Bioconductor package for differential expression analysis of digital gene expression data.* Bioinformatics, 2010. **26**(1): p. 139-140.

33. Love, M.I., W. Huber, and S. Anders, *Moderated estimation of fold change and dispersion for RNA-seq data with DESeq2.* Genome Biol,

2014. **15**(12): p. 550.

34. Huang, D.W., B.T. Sherman, and R.A. Lempicki, *Systematic and integrative analysis of large gene lists using DAVID bioinformatics resources.* Nature Protocols, 2009. **4**(1): p. 44-57.

35. de Hoon, M.J., et al., *Open source clustering software.* Bioinformatics, 2004. **20**(9): p. 1453-4.

36. Saldanha, A.J., *Java Treeview-extensible visualization of microarray data.* Bioinformatics, 2004. **20**(17): p. 3246-3248.

37. Mascarenhas, J. and R. Hoffman, *Ruxolitinib: The First FDA Approved Therapy for the Treatment of Myelofibrosis.* Clinical Cancer Research, 2012. **18**(11): p. 3008-3014.

38. Cokol-Cakmak, M., et al., *Diagonal Method to Measure Synergy Among Any Number of Drugs.* Jove-Journal of Visualized

Experiments, 2018(136).

39. Foucquier, J. and M. Guedj, *Analysis of drug combinations: current methodological landscape.* Pharmacology Research & Perspectives, 2015. **3**(3).

40. Tsuyada, A., et al., *CCL2 Mediates Cross-talk between Cancer Cells and Stromal Fibroblasts That Regulates Breast Cancer Stem Cells.* Cancer Research, 2012. **72**(11): p. 2768-2779.

41. Bochet, L., et al., *Cancer-associated adipocytes promotes breast tumor radioresistance.* Biochemical and Biophysical Research Communications, 2011. **411**(1): p. 102-106.

42. Wang, L., et al., *Targeting HDAC with a novel inhibitor effectively reverses paclitaxel resistance in non-small cell lung cancer via multiple mechanisms.* Cell Death & Disease, 2016. **7**.

43. Bae, T., et al., *Restoration of paclitaxel resistance by CDK1 intervention in drug-resistant ovarian cancer.* Carcinogenesis, 2015. **36**(12): p. 1561-1571.

44. Mi, Y.J., et al., *Apatinib (YN968D1) Reverses Multidrug Resistance by Inhibiting the Efflux Function of Multiple ATP-Binding Cassette Transporters.* Cancer Research, 2010. **70**(20): p. 7981-7991.

45. Ruan, Z.Y., X.Y. Yang, and W.W. Cheng, *OCT4 accelerates tumorigenesis through activating JAK/STAT signaling in ovarian cancer side population cells.* Cancer Management and Research, 2019. **11**: p. 389-398.

46. Khanna, P., et al., *GRAMD1B regulates cell migration in breast cancer cells through JAK/STAT and Akt signaling.* Scientific Reports, 2018. **8**.

47. Zhu, D.Y., et al., *Long noncoding RNA PART1 promotes progression of non-small cell lung cancer cells via JAK-STAT signaling pathway.* Cancer Medicine, 2019.

48. Burke, W.M., et al., *Inhibition of constitutively active Stat3 suppresses growth of human ovarian and breast cancer cells.* Oncogene, 2001. **20**(55): p. 7925-34.

49. Alvarez, J.V., et al., *Identification of a genetic signature of activated signal transducer and activator of transcription 3 in human tumors.* Cancer Research, 2005. **65**(12): p. 5054-5062.

50. Walker, S.R., et al., *Reciprocal Effects of STAT5 and STAT3 in Breast Cancer.* Molecular Cancer Research, 2009. **7**(6): p. 966-976.

51. Marotta, L.L.C., et al., *The JAK2/STAT3 signaling pathway is required for growth of CD44(+)CD24(-) stem cell-like breast*

cancer cells in human tumors. Journal of Clinical Investigation, 2011. **121**(7): p. 2723-2735.

52. Banerjee, K. and H. Resat, *Constitutive activation of STAT3 in breast cancer cells: A review.* International Journal of Cancer, 2016. **138**(11): p. 2570-2578.

53. Walker, S.R., M. Xiang, and D.A. Frank, *Distinct roles of STAT3 and STAT5 in the pathogenesis and targeted therapy of breast cancer.* Mol Cell Endocrinol, 2014. **382**(1): p. 616-621.

54. Cui, Y., et al., *Inactivation of Stat5 in mouse mammary epithelium during pregnancy reveals distinct functions in cell proliferation, survival, and differentiation.* Molecular and Cellular Biology, 2004. **24**(18): p. 8037-8047.

55. Iavnilovitch, E., B. Groner, and I. Barash, *Overexpression and forced*

activation of Stat5 in mammary gland of transgenic mice promotes cellular proliferation, enhances differentiation, and delays postlactational apoptosis. Molecular Cancer Research, 2002. **1**(1): p. 32-47.

56. Caffarel, M.M., et al., *Constitutive activation of JAK2 in mammary epithelium elevates Stat5 signalling, promotes alveologenesis and resistance to cell death, and contributes to tumourigenesis.* Cell Death Differ, 2012. **19**(3): p. 511-22.

57. Li, X., et al., *Reverse of microtubule-directed chemotherapeutic drugs resistance induced by cancer-associated fibroblasts in breast cancer.* Onco Targets Ther, 2019. **12**: p. 7963-7973.

58. Kim, J.W., et al., *Inhibition of tumor growth and angiogenesis of tamoxifen-resistant breast cancer cells by ruxolitinib, a selective*

JAK2 inhibitor. Oncol Lett, 2019. **17**(4): p. 3981-3989.

국문초록

유방암은 전 세계적으로 여성암 중 가장 높은 비율을 차지하고 있으며, 한국에서는 유방암의 발병률이 해마다 꾸준히 증가하고 있다. 삼중 음성 유방암은 여러가지 아형 유방암 중 가장 악성이며 치료하기가 가장 어려운 유형이다. 다른 아형 유방암에서는 호르몬 요법을 통해 estrogen 수용체, progesterone 수용체, 그리고 HER2 수용체 중 하나를 표적으로 하여 치료하지만, 삼중 음성 유방암의 경우 이러한 수용체 분자가 존재하지 않기 때문에 치료가 어려우며 보통 항암치료를 동반하게 된다. 파클리탁셀은 유방암의 치료에 대표적인 항암제 중 하나이지만, 항암치료를 하는 과정에서 파클리탁셀에 대한 내성을 획득하기도 하며, 이러한 항암제에 대한 내성은 유방암의 치료에 있어 여전히 큰 문제 중 하나이다. 따라서 본 연구는 삼중 음성 유방암에서 어떠한 기작으로 파클리탁셀에 대한 내성이 발생하는지를 알아보기 위해 7가지 삼중 음성 유방암 환자유래조직 모델을 이용하여 파클리탁셀에 대한 반응성을 평가하였다. 각각의 삼중 음성 유방암 환자유래조직 모델들은 대조군과 파클리탁셀 투여군으로 구성되었고, PBS 또는 파클리탁셀을 15mg/kg으로 4주간 복강 내 주사로 투여한 후 파클리탁셀에 대한 종양크기의 감소율을 비교 분석하였다. 상대적으로 파클리탁셀에 의한 반응성이 적은 4가지 삼중 음성 유방암

환자유래조직 모델을 파클리탁셀 저항성 군으로 정하였고, 파클리탁셀에 의한 반응성이 큰 3가지 삼중 음성 유방암 환자유래조직 모델을 파클리탁셀 반응성 군으로 정하였다. 그리고 파클리탁셀 저항성 군과 파클리탁셀의 반응성 군의 전사체와 유전체 시퀀싱 분석을 통해 어떠한 유전자들의 발현 차이를 비교분석하였다. 그 결과 파클리탁셀에 저항성을 가지는 군에서 JAK-STAT pathway와 관련된 유전자의 발현이 파클리탁셀에 반응성을 가지는 군들에 비해 상대적으로 증가되어 있는 것을 확인하였다. 따라서 JAK-STAT pathway의 활성에 의해 파클리탁셀에 저항성을 가질 것이라는 가설을 세웠다. 따라서 파클리탁셀 저항성을 가지는 군의 종양과 파클리탁셀 반응성을 가지는 군의 종양에서 단백질을 추출하여 JAK-STAT pathway와 관련된 단백질들의 발현량과 이들의 활성을 비교 분석하였다. 그 결과 전사체 시퀀싱 분석의 결과와 유사하게 단백질 수준에서도 JAK-STAT pathway 관련 단백질들의 발현량이 증가한 것을 확인할 수 있었다. 이를 유방암 세포에 적용시키기 위해, qPCR와 western blot을 통해 JAK-STAT pathway가 활성이 되어 있는 삼중 음성 유방암 세포들을 선별하였다. 그리고 선별된 삼중 음성 유방암 세포들에서 JAK1과 JAK2의 저해제인 룩소리티닙과 파클리탁셀을 동시에 처리하여 상승효과를 확인하였으며, 또한 JAK2를 siRNA를 이용하여 발현을 억제하였을 때, 파클리탁셀에 의한 항암작용이 증가되는 것을 확인하였다. 따라서 삼중

음성 유방암에서 JAK-STAT pathway의 활성이 파클리탁셀의 반응성에 영향을 미치는 것을 알 수 있었다. 그리고 JAK-STAT pathway는 종양 이외에 종양 주변의 미세환경에 영향을 준다는 기존의 연구결과가 많이 보고되었다. 따라서 JAK-STAT pathway가 종양 주변 미세환경에 어떠한 영향을 주는지 알아보기 위하여, 마우스의 DEG를 분석하였을 때, cell cycle과 관련된 유전자들의 발현량이 파클리탁셀 저항성을 가지는 군에서 증가되어 있는 것을 알 수 있었다. 그리고 면역염색을 통해 파클리탁셀 저항성을 가지는 종양 주변의 미세환경을 구성하는 fibroblast와 endothelial cell에서 세포증식이 증가하는 것을 확인하였다. 또한 JAK2가 억제된 conditioned media에서 키운 마우스의 fibroblast의 증식이 억제되는 것을 확인하였다. 따라서 삼중 음성 유방암에서 JAK-STAT pathway의 활성이 종양 주변의 미세환경 구성하는 fibroblast 또는 endothelial cell과 같은 세포들의 증식을 조절함으로써 파클리탁셀에 대한 반응성에 영향을 준다는 것을 알 수 있었다. 이를 바탕으로 파클리탁셀에 내성이 있는 삼중음성 유방암의 잠재적인 치료의 가능성을 제시하였다,

주요어: 삼중음성 유방암, 파클리탁셀, 저항성, JAK-STAT pathway, 암조직

주변 미세환경

학 번: 2018-27894